

# Reconfigurable Intelligent Surface for Vehicular Communications: Exact Performance Analysis with Phase Noise and Mobility

Vinay Kumar Chapala, *Graduate Student Member, IEEE* and S. M. Zafaruddin, *Senior Member, IEEE*

**Abstract**—Recent research provides an approximation on the performance for reconfigurable intelligent surface (RIS) assisted systems over generalized fading channels with phase noise resulting from imperfect phase compensation at the RIS. This paper presents an exact analysis of RIS-assisted vehicular communication by coherently combining received signals reflected by RIS elements and direct transmissions from the source terminal, considering generalized fading channels and phase noise. We adopt the generalized uniform distribution to model the phase noise resulting from a finite set of phase shifts at the RIS. We use generalized- $K$  shadowed fading distribution for the direct link and asymmetrical channels for the RIS-assisted transmission with  $\kappa$ - $\mu$  distribution for the first link and double generalized Gamma (dGG) distribution for the second link combined with a statistical random way point (RWP) model for the destination under movement. We employ a novel approach to represent the probability density function (PDF) and cumulative distribution function (CDF) of the product of four channel coefficients in terms of a single univariate Fox's H-function, and develop an exact statistical analysis of the end-to-end signal-to-noise ratio (SNR) for the considered system using multi-variate Fox's H-function. We also use the inequality between the arithmetic and geometric mean to simplify the statistical results of the considered system in terms of the univariate Fox's H-function. We present exact, upper bound, and asymptotic expressions of the outage probability and average bit-error-rate (BER) performance using the derived density and distribution functions. We validate the analytical expressions through numerical and simulation results and demonstrate the effect of phase noise and mobility on the performance scaling with RIS elements and direct transmissions considering various practically relevant scenarios.

**Index Terms**—Bit error rate, Fox's H-function, mobility, outage probability, phase noise, reconfigurable intelligent surface (RIS), vehicular networks.

## I. INTRODUCTION

The upcoming 6G wireless system envisions to cater exceedingly higher requirements of network throughput, lower latency of transmission, and stable connectivity for autonomous vehicular communications [2]. However, dynamic channel conditions between an access point to a vehicle

in motion may be a bottleneck for the desired quality of service. The use of reconfigurable intelligent surface (RIS) can be a promising technology to create a strong line-of-sight (LOS) transmissions by artificially controlling the characteristics of propagating signals for vehicular communications [2]–[4]. An RIS is a planar metasurface made up of a large number of inexpensive passive reflective elements that can be electronically programmed to customize the phase of the incoming electromagnetic wave for enhanced signal quality and transmission coverage.

At the outset, related research assumed ideal phase compensation at the RIS module to analyze the performance of RIS empowered wireless networks such as radio-frequency (RF) [5]–[11], free-space optics (FSO) [12], [13], terahertz (THz) [14], [15], and vehicular [16]–[21]. Under the assumption of the ideal phase, statistical characterization of the RIS-assisted system requires the derivation for the sum of the product of two fading coefficients corresponding to the two links between the source to the RIS and RIS to the destination. Initially, the research works applied the central limit theorem (CLT) to develop approximate analysis for various fading models [5]–[8], [16]. Recently, the authors in [10], [13]–[15] used the multivariate Fox's H-function representation to develop an exact analysis of various RIS-assisted wireless networks. The authors in [10] presented an exact performance analysis for RIS-assisted wireless transmissions over generalized Fox's H fading channels. The authors in [14], [15] analyzed RIS-aided THz communications over different fading channel models combined with antenna misalignment and hardware impairments. In [13], a unified performance analysis for a FSO system was presented considering different atmospheric turbulence models and pointing errors. In the conference version of the paper, we presented an exact analysis for RIS-aided transmissions with direct link over double generalized (dGG) fading that accurately models the vehicular communications [1].

It should be emphasized that the above and related research assumed ideal phase compensation at the RIS to facilitate performance analysis. However, phase noise resulting from imperfect phase compensation at the RIS is inevitable in a practical setup. The impact of phase noise becomes of a paramount importance, especially in vehicular communications considering the dynamics of channel between the RIS and the destination under movement. Generally, the phase noise is statistically distributed as Gaussian or generalized uniform [22]. Under the statistical phase noise, performance

A preliminary version of the paper without phase noise and mobility with symmetric dGG fading channel was presented at the 2022 IEEE 95th Vehicular Technology Conference (VTC2022-Spring), Helsinki, Finland, 19-22 June 2022 [1].

This work was supported in part by the Science and Engineering Research Board (SERB), Government of India, under MATRICS Grant MTR/2021/000890 and Start-up Research Grant SRG/2019/002345.

Vinay Kumar Chapala (p20200110@pilani.bits-pilani.ac.in) and S. M. Zafaruddin (syed.zafaruddin@pilani.bits-pilani.ac.in) are with the Department of Electrical and Electronics Engineering, Birla Institute of Technology and Science, Pilani, Pilani Campus, Pilani-333031, Rajasthan, India.

TABLE I  
RELATED RESEARCH WITH PHASE NOISE

Ref	Direct Link	Mobility	RIS Channels	Fading Types	Analysis
[23]	No	No	Symmetric	(Rayleigh, Rayleigh)	CLT
[29]	No	No	Symmetric	(General, General)	Approximation
[24]	Yes	No	Symmetric	(Rayleigh, Rayleigh)	CLT
[25]	Yes	No	Symmetric	(Rayleigh, Rayleigh)	CLT
[27]	No	No	Symmetric	(Rician, Rician)	Approximation
[22]	No	No	Symmetric	(Fox-H, Fox-H)	CLT, lower and upper bounds
[28]	No	No	Symmetric	(Nakagami-m, Nakagami-m)	Exact for integer $m$
This Paper	Yes	Yes	Asymmetric	( $\kappa$ - $\mu$ , dGG)	Exact and Bounds

of RIS-assisted wireless system requires the analysis for the sum of the product of three fading coefficients. As is for perfect phase compensations, existing works approximate the performance of RIS system for various fading channels in the presence of phase noise [5], [23]–[28]. In [5], [23], [24], [25], authors applied the CLT to analyze the performance of RIS system over Rayleigh fading channel with phase errors. The authors in [29] approximated an arbitrary fading model with Nakagami- $m$  distributed to develop performance analysis of the RIS-assisted transmission with phase noise. The reference [26] studied the effect of quantization level of the phase noise on the diversity order of the system. The authors in [27] derived approximate performance bounds for Rician fading model with phase errors.

It is desirable to provide an exact analysis for RIS-assisted system in the presence of phase noise for a better performance assessment. In [28], the authors derived exact statistical analysis for RIS-assisted system over Nakagami- $m$  fading channel with phase noise. However, the analysis is valid for integer values of fading parameter  $m$  and may approximate the performance of the system when the parameter  $m$  becomes real. Similar to the case for perfect phase compensation, it is natural to apply the multivariate Fox's H-function to represent the analysis with the phase noise in an exact form. However, an application of the theory of random variables for the product of three channel coefficients with generalized fading models results into bivariate Fox's H-function. However, statistical representation of the sum of bivariate Fox's H-functions is intractable mathematically. Recently, the authors in [22] provided an exact analytical expression using multivariate Fox's H-function for RIS-assisted system with generalized fading models without phase noise but provided approximate analysis in the presence of phase noise. For vehicular communications, the phase noise at the RIS module should not be neglected considering the dynamics of the channel due to the mobility effect. Moreover, the two links from source to RIS and RIS to destination may not incur symmetrical fading. Furthermore, direct link with the combined effect of fading and shadowing should be included in the analysis. To the best of the author's knowledge, an exact analysis of RIS-assisted wireless transmission with phase noise and user mobility over asymmetrical and generalized fading channels considering the shadowed direct link has not been studied yet. A summary of related research on the topic has been provided in Table (I).

In this paper, we analyze the performance of RIS-assisted vehicular communication system by coherently combining

received signals reflected by RIS elements and direct transmissions from the source terminal, considering generalized fading channels and phase noise. The major contributions of the paper are listed as follows:

- We adopt the generalized uniform distribution to model statistically the phase noise resulting from a finite set of phase shifts at the RIS.
- We use generalized- $K$  shadowed fading distribution for the direct link and asymmetrical channels for the RIS-assisted transmission with  $\kappa$ - $\mu$  distribution for the first link and double generalized Gamma (dGG) distribution for the second link combined with a statistical random way point (RWP) model for the destination under movement.
- We employ a novel approach to represent the probability density function (PDF) and cumulative distribution function (CDF) of the product of four channel coefficients in terms of a single univariate Fox-H function. We use the derived PDF to develop an exact statistical analysis of the end-to-end signal-to-noise ratio (SNR) for the RIS-assisted system using multi-variate Fox-H function. Further, we use the inequality between the arithmetic and geometric mean to simplify the statistical results of the considered system in terms of the univariate Fox-H function.
- We present exact, upper bound, and asymptotic expressions of the outage probability and average bit-error-rate (ABER) performance using the derived density and distribution functions for better Engineering insights on the system performance at a high SNR.
- We validate the analytical expressions through numerical and simulation results and demonstrate the effect of phase noise and mobility on the performance scaling with RIS elements and direct transmissions considering various practically relevant scenarios.

#### Description of Main Notations:

Main notations used in this paper are as follows:  $j$  denotes the imaginary number,  $\mathbb{E}[\cdot]$  denotes the expectation operator,  $\exp(\cdot)$  denotes the exponential function, while  $\Gamma(a) = \int_0^\infty u^{a-1} e^{-u} du$  denotes the Gamma function. We denote the Meijer's G-function by  $G_{p,q}^{m,n} \left( x \left| \begin{matrix} \{a_w\}_{w=1}^p \\ \{b_w\}_{w=1}^q \end{matrix} \right. \right)$ , the single-variate Fox's H-function by  $H_{p,q}^{m,n} \left( x \left| \begin{matrix} \{(a_w, A_w)\}_{w=1}^p \\ \{(b_w, B_w)\}_{w=1}^q \end{matrix} \right. \right)$ ,  $N$ -variate Fox's H-function as defined in [30, A.1] and a

shorthand notation  $\{a_i\}_1^N = \{a_1, \dots, a_N\}$  to represent their coefficients.

### Organization of the Paper:

This paper is organized as follows: In Section II, we describe the system with channel fading models. In Section III, we develop statistical results for RIS-assisted transmission with phase noise and mobility. In Section IV, we analyze the performance of considered system using outage probability and average BER. In Section V, numerical and simulation results are presented. Section VI concludes the paper.

## II. SYSTEM MODEL

We consider a transmission model, where a single antenna source communicates with a destination equipped with a single antenna through an RIS with  $N$  reflecting elements as shown in Fig. 1. We consider that the elements of RIS are spaced half of the wavelength and assume independent channels at the RIS [4], [11], [31]. We denote  $h_i^{(f)} = |h_i^{(f)}|e^{j\theta_{h_i}}$  and  $g_i^{(f)} = |g_i^{(f)}|e^{j\theta_{g_i}}$  are channel fading coefficients between the source to the  $i$ -th RIS element and between the  $i$ -th RIS element to the destination, respectively. Assuming flat fading channel and imperfect phase compensation, the residual phase is non-zero,  $\phi_i = -\theta_{h_i} - \theta_{g_i} + \theta_i$ , where  $\theta_i$  is random phase noise,  $\theta_{h_i}$  is the phase of the first link, and  $\theta_{g_i}$  is the phase of the second link. Thus, the received signal becomes

$$y = \sqrt{P_t}x \left( \sum_{i=1}^N H_{l,i} h_i^{(f)} g_{i,i}^{\text{rwp}} g_i^{(f)} e^{j\phi_i} + \omega h_{l,d}^{\text{rwp}} h_d^{(f)} \right) + v \quad (1)$$

where  $P_t$  is the transmit power,  $x$  is the unit power information bearing signal,  $|h_i^{(f)}|$  and  $|g_i^{(f)}|$  are channel fading coefficients between the source to the  $i$ -th RIS element and between the  $i$ -th RIS element to the destination, respectively,  $|h_d^{(f)}|$  is the flat fading coefficient between source and destination, and  $v$  is the additive Gaussian noise with zero mean and variance  $\sigma_v^2$ . The terms  $H_{l,i}$ ,  $g_{l,i}$  and  $h_{l,d}$  denote the path loss coefficients from source to RIS, RIS to destination and source to destination respectively. We denote  $g_i = g_{l,i}|g_i^{(f)}|$  and for direct link,  $h_d = h_{l,d}|h_d^{(f)}|$ . Here,  $\omega = 1$  depicts the scenario with direct link and  $\omega = 0$  corresponds to the case without the direct link. Let  $d_1$  and  $d_2$  be the distances from source to RIS and RIS to destination. The distance from source to destination is considered as  $d = \sqrt{d_1^2 + d_2^2}$ . The path loss component from source to RIS is considered as  $H_{l,i} = d_1^{-\frac{a}{2}} \left( \frac{c}{4\pi f_c} \right)$ , where  $a$  is the path loss exponent,  $c$  is the speed of the light and  $f_c$  is the carrier frequency.

### A. Fading Models

We assume that RIS is placed close to the source and destination is relatively far from the RIS and hence both the links may undergo asymmetrical fading. Most of the existing studies model the RF link as Rayleigh, Nakagami- $m$ , or Rician fading. These channel models may not be an actual representation of fading characteristics of the RF link. The use of line-of-sight (LOS) based fading models are more suitable

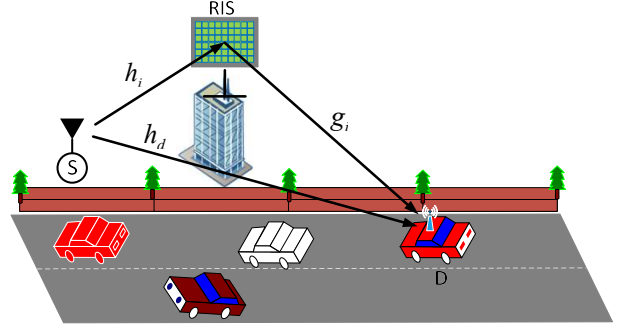


Fig. 1. System Model.

for RIS transmission. The  $\kappa$ - $\mu$  fading model is a generalized LOS model fits well with experimental data over a wide range of scenarios [32]. The  $\kappa$ - $\mu$  contains Nakagami- $m$  ( $\kappa \rightarrow 0$ ,  $\mu = m$ ) model and the well studied Rician ( $\mu = 1$ ) fading channel for RIS-assisted transmission as a particular case.

We consider the channel from source to RIS  $|h_i^{(f)}|$  distributed as  $\kappa$ - $\mu$  with the PDF [32]

$$f_{|h_i^{(f)}|}(x) = \frac{2\mu_i(1+\kappa_i)^{\frac{1+\mu_i}{2}} x^{\mu_i} \exp\left[-\mu_i(1+\kappa_i)x^2\right]}{\kappa_i^{\frac{\mu_i-1}{2}} \exp(\mu_i\kappa_i)} I_{\mu_i-1}\left[2\mu_i\sqrt{\kappa_i(1+\kappa_i)}x\right] \quad (2)$$

where  $\kappa_i$  is the ratio of power of the dominant components and the total power of scattered waves and  $I_v(x)$  is the modified Bessel function of the first kind of order  $v$  and can be represented by its infinite series as  $I_v(x) = \sum_{k=0}^{\infty} \frac{1}{k!(v+k+1)} \left(\frac{x}{2}\right)^{v+2k}$ . Using the series expansion and after some algebraic manipulations, we get

$$f_{|h_i^{(f)}|}(x) = \sum_{k_i=0}^{\infty} \psi_{i,1} x^{\mu_i+k_i-1} e^{-\zeta_{i,1}x} \quad (3)$$

where  $\psi_{i,1} = \frac{1}{k_i!(\mu_i+k_i)} \frac{\mu_i^{\mu_i+2k_i} \kappa_i^{k_i} (1+\kappa_i)^{\mu_i+k_i}}{\exp(\mu_i\kappa_i)}$  and  $\zeta_{i,1} = \mu_i(1+\kappa_i)$ . We model the channel between the RIS to the destination  $|g_i^{(f)}|$  distributed as double Generalized-Gamma (dGG) with the PDF [33]:

$$f_{|g_i^{(f)}|}(x) = \frac{1}{\Gamma(\beta_{i,1})\Gamma(\beta_{i,2})} x^{-1} H_{0,2}^{2,0} \left[ \phi_{g,i}^{\frac{1}{\alpha_{i,2}}} x \mid (\beta_{i,2}, \frac{1}{\alpha_{i,2}}), (\beta_{i,1}, \frac{1}{\alpha_{i,1}}) \right] \quad (4)$$

where  $\phi_{g,i} = \frac{\beta_{i,2}}{\Omega_{i,2}} \left( \frac{\beta_{i,1}}{\Omega_{i,1}} \right)^{\frac{\alpha_{i,2}}{\alpha_{i,1}}}$ ,  $\alpha_{i,1}$ ,  $\beta_{i,1}$ ,  $\alpha_{i,2}$ ,  $\beta_{i,2}$  are Gamma distribution shaping parameters and  $\Omega_{i,j} = \left( \frac{\mathbb{E}[x_{i,j}^2] \Gamma(\beta_{i,j})}{\Gamma(\beta_{i,j}+2/\alpha_{i,j})} \right)^{\alpha_{i,j}/2}$ ,  $j = 1, 2$  is the  $\alpha_{i,j}$ -root mean value. The dGG model is suitable for modeling non-homogeneous double-scattering radio propagation fading conditions for vehicular communications over RF frequencies [34]. The dGG is a generalized model which contains most of the existing statistical models such as double-Nakagami, double-Rayleigh, double Weibull, and Gamma-Gamma as special cases.

We use the generalized  $\mathcal{K}$  distribution to model the direct channel  $|h_d^{(f)}|$  from  $S$  to  $D$  under the combined effect of short term fading and shadowing [35]

$$f_{|h_d^{(f)}|}(x) = \frac{2b}{\Gamma(m)\Gamma(M)} \left( \frac{bx}{2} \right)^{M+m-1} K_{M-m}(bx) \quad (5)$$

where  $b = 2\sqrt{\frac{m}{m_0}}$  and  $K_{M-m}(\cdot)$  is the modified bessel function of second kind of the order  $(M - m)$ . Here,  $M = \frac{1}{\exp(\sigma_n^2) - 1}$ ,  $\sigma_n > 0$  denotes the severity of shadowing with factor  $\sigma_{\text{dB}} = 8.686\sigma_n$ ,  $m > 0$  is frequency dependent parameter characterizing the small-scale fading, and  $m_0$  is a measure of mean power.

We express  $K_{M-m}(bx)$  in terms of Meijer G-function as  $K_{M-m}(x) = \frac{1}{2}G_{0,2}^{2,0}\left(\frac{b^2x^2}{4} \mid \frac{M-m}{2}, \frac{m-M}{2}\right)$  to get

$$f_{|h_d^{(f)}|}(x) = \frac{b}{\Gamma(m)\Gamma(M)}\left(\frac{bx}{2}\right)^{M+m-1} G_{0,2}^{2,0}\left[\frac{b^2x^2}{4} \mid \frac{M-m}{2}, \frac{m-M}{2}\right] \quad (6)$$

### B. Statistical Models for Phase Noise and Mobility

In the literature, there are three different models, Gaussian, generalized uniform and uniform RVs for phase noise [22]. In the practical setup, due to hardware limitations, only a finite set of phase shifts can be realized that lead to quantization errors. To this extent, in our analysis, we consider generalized uniform distribution i.e.,  $\theta_i \sim U(-q\pi, q\pi)$  that models the quantization noise for  $q = 2^{-L}$ , where  $L \geq 1$  denotes the number of quantization bits. It should be noted that assumption of perfect phase compensation may not be appropriate for vehicular communications.

We use the RWP model to consider the effect of mobility in the RIS to destination link [36]. The average received power in general depends on the propagation distance as  $P_t r^{-a}$ , where  $P_t$  is the transmit power and  $a$  ( $2 \leq a \leq 5$ ) is the path-loss exponent that depends on the propagation environment. For the static user, the path loss component  $r^{-a}$  is constant but for a moving user, the distance  $r$  is a random variable. In the RWP mobility model, it is usually assumed that the receiving users are located at randomly selected coordinate points in the vicinity of the transmitter, which depends on the network topology. For a 1-D topology, we consider a line with the transmitter being located at the origin. The 2-D topology is assumed to be a circle, whereas a 3-D topology is a spherical network. In both the 2-D and 3-D network topologies, it is assumed that the transmitter is located at the origin. The RWP mobility models are polynomials in the transmitter-receiver distance  $r$ , and the PDF of the distance  $r$  is given by the general form [36]

$$f_r(x) = \sum_{j=1}^n B_j \frac{r^{\beta_j}}{d^{\beta_j+1}} \quad (7)$$

where parameters  $n$ ,  $B_j$ , and  $\beta_j$  depend on the number of dimensions considered in the topology summarized in [36]. For example, [36, Table I] gives  $n = 2, B_j = [6, -6]$ , and  $\beta_j = [1, 2]$  for 1-D topology;  $n = 3, B_j = (\frac{1}{73}) \times [324, -420, 96]$ , and  $\beta_j = [1, 3, 55]$  for 2-D topology; and  $n = 3, B_j = (\frac{1}{72}) \times [735, -1190, 455]$ , and  $\beta_j = [2, 4, 6]$  for 3-D topology. The authors in [17], [37] also employed RWP model for analyzing the performance of RIS system for the user under mobility.

### III. STATISTICAL DERIVATIONS

In this section, we develop probability density and distribution functions for the effective channel for RIS-assisted transmission with phase noise and mobility. Without the loss of generality, we assume  $H_{l,i} = H_l, \forall i$ , and rewrite (1) as:

$$y = \sqrt{P_t}x \left( H_l \sum_{i=1}^N Z_i + \omega Z_d \right) + v \quad (8)$$

where  $Z_i = |h_i^{(f)}| |g_{l,i}^{\text{rwp}}| |g_i^{(f)}| e^{j\theta_i}$  is the product of four random variables and  $Z_d = h_{l,d}^{\text{rwp}} |h_d^{(f)}|$  is the product of two random variables.

#### A. Without Direct Link ( $\omega = 0$ )

We use the multivariate Fox's H-function to develop exact expressions of the PDF and CDF for  $Z_{\text{RIS}} = \sum_{i=1}^N Z_i$ . We also present bounds on analytical expressions for RIS-assisted transmission using univariate Fox's H-function for better insights into the system performance.

Since  $Z_i$  is the product of four random variables with complicated distribution functions, a straight forward application of the probability theory may lead the PDF of  $Z_i$  in terms bivariate/trivariate Fox's H-function, precluding the representation of  $Z_{\text{RIS}} = \sum_{i=1}^N Z_i$  using multivariate Fox's H-function. In the following Theorem, we apply a novel approach to derive the PDF  $Z_i$  in terms of univariate Fox's H-function:

**Theorem 1.** *The PDF of effective channel  $Z_i$  for a single-element RIS under the combined effect of generalized asymmetric channels, user mobility, and phase errors is given as*

$$f_{Z_i}(x) = \sum_{k_i=0}^{\infty} \sum_{j_i=1}^n \psi_i x^{-1} H_{2,5}^{3,1} \left[ \zeta_{i,1} \zeta_{i,2} x \mid \begin{matrix} (-\beta_{j_i}, \frac{a}{2}), (1, q) \\ V_i, (0, q) \end{matrix} \right] \quad (9)$$

where  $\psi_i = \psi_{i,1} \psi_{i,2} \zeta_{i,1}^{-(\mu_i+k_i)}$ ,  $V_i = (\beta_{i,2}, \frac{1}{\alpha_{i,2}}), (\beta_{i,1}, \frac{1}{\alpha_{i,1}}), (\mu_i + k_i, 1), (-1 - \beta_{j_i}, \frac{a}{2})$ .

*Proof:* See Appendix A. ■

As a special case, we can consider i.n.i.d. Rayleigh fading in both the hops from source to RIS and RIS to destination by substituting  $\kappa = 0$  and  $\mu = 1$  in (2), and  $\alpha_1 = 1$  and  $\beta_1 = 2$  in (4) to simplify PDF expressions for fading channels. Applying the similar approach for the proof of Theorem 1, we can get the PDF of  $Z_i$  for Rayleigh fading channel with phase noise and mobility:

$$f_{Z_i}(x) = \sum_{j_i=1}^n B_{j_i} x^{-1} H_{2,4}^{2,1} \left[ \frac{2}{\Omega_{i,1}} d_2^{\frac{a}{2}} x \mid \begin{matrix} (-\beta_{j_i}, \frac{a}{2}), (1, q) \\ (2, 1), (1, 1), (-1 - \beta_{j_i}, \frac{a}{2}), (0, q) \end{matrix} \right] \quad (10)$$

Further, we can simplify (10) by neglecting the mobility effect to get the PDF of  $Z_i$  for Rayleigh fading channel with phase noise:

$$f_{Z_i}(x) = x^{-1} H_{1,3}^{2,1} \left[ \frac{2}{\Omega_{i,1}} x \mid \begin{matrix} (1, q) \\ (2, 1), (1, 1), (0, q) \end{matrix} \right] \quad (11)$$

In what follows, we use the univariate Fox's H-function representation for the PDF of  $Z_i$  in Theorem 1 to develop

statistical results for  $Z_{\text{RIS}} = \sum_{i=1}^N Z_i$  in the following Lemma:

**Lemma 1.** *The PDF and CDF of the resultant RIS channel  $Z_{\text{RIS}} = \sum_{i=1}^N Z_i$  are given by*

$$f_{Z_{\text{RIS}}}(x) = \sum_{k_1, \dots, k_N=0}^{\infty} \sum_{j_1, \dots, j_N=1}^n \prod_{i=1}^N \psi_i x^{-1} H_{0,1:3,5; \dots; 3,5}^{0,0:3,2; \dots; 3,2} \left[ \left\{ \zeta_{i,1} \zeta_{i,2} x \right\}_1^N \mid - : \left\{ (-\beta_{j_i}, \frac{a}{2}), (1, q), (1, 1) \right\}_{i=1}^N \right] \quad (12)$$

$$F_{Z_{\text{RIS}}}(x) = \sum_{k_1, \dots, k_N=0}^{\infty} \sum_{j_1, \dots, j_N=1}^n \prod_{i=1}^N \psi_i H_{0,1:3,5; \dots; 3,5}^{0,0:3,2; \dots; 3,2} \left[ \left\{ \zeta_{i,1} \zeta_{i,2} x \right\}_1^N \mid - : \left\{ (-\beta_{j_i}, \frac{a}{2}), (1, q), (1, 1) \right\}_{i=1}^N \right] \quad (13)$$

where  $V_i = (\beta_{i,2}, \frac{1}{\alpha_{i,2}}), (\beta_{i,1}, \frac{1}{\alpha_{i,1}}), (\mu_i + k_i, 1), (-1 - \beta_{j_i}, \frac{a}{2})$ .

*Proof:* See Appendix B. ■

Similarly, we can use (10) in Lemma 1 to develop the PDF and CDF of  $Z_{\text{RIS}}$  for Rayleigh fading with user mobility and phase noise:

$$f_{Z_{\text{RIS}}}(x) = \sum_{j_1, \dots, j_N=1}^n \prod_{i=1}^N B_{j_i} x^{-1} H_{0,1:3,4; \dots; 3,4}^{0,0:2,2; \dots; 2,2} \left[ \left\{ \frac{2}{\Omega_{i,1}} d_2^{\frac{a}{2}} x \right\}_1^N \mid - : \left\{ (-\beta_{j_i}, \frac{a}{2}), (1, q), (1, 1) \right\}_{i=1}^N \right] \quad (14)$$

$$F_{Z_{\text{RIS}}}(x) = \sum_{j_1, \dots, j_N=1}^n \prod_{i=1}^N B_{j_i} H_{0,1:3,4; \dots; 3,4}^{0,0:2,2; \dots; 2,2} \left[ \left\{ \frac{2}{\Omega_{i,1}} d_2^{\frac{a}{2}} x \right\}_1^N \mid - : \left\{ (-\beta_{j_i}, \frac{a}{2}), (1, q), (1, 1) \right\}_{i=1}^N \right] \quad (15)$$

where  $V_i = (2, 1), (1, 1), (-1 - \beta_{j_i}, \frac{a}{2})$ .

Further, we can use (11) in Lemma 1 to represent the PDF and CDF of  $Z_{\text{RIS}}$  for Rayleigh fading channels with phase noise as

$$f_{Z_{\text{RIS}}}(x) = x^{-1} H_{0,1:2,3; \dots; 2,3}^{0,0:2,1; \dots; 2,1} \left[ \left\{ \frac{2}{\Omega_{i,1}} x \right\}_1^N \mid - : \left\{ (1, q), (1, 1) \right\}_{i=1}^N \right] \quad (16)$$

$$F_{Z_{\text{RIS}}}(x) = H_{0,1:2,3; \dots; 2,3}^{0,0:2,1; \dots; 2,1} \left[ \left\{ \frac{2}{\Omega_{i,1}} x \right\}_1^N \mid - : \left\{ (1, q), (1, 1) \right\}_{i=1}^N \right] \quad (17)$$

where  $V_i = (2, 1), (1, 1), (-1 - \beta_{j_i}, \frac{a}{2})$ .

Although computational routines [38] are available for multivariate Fox's H-function in Lemma 1, it is desirable to simplify the analytical expressions using univariate Fox's H-function for better insights into the system performance.

Using the inequality of arithmetic mean and geometric mean, we can express  $\sum_{i=1}^N \frac{Z_i}{N} \geq \prod_{i=1}^N Z_i^{\frac{1}{N}}$ . Thus, an upper bound on the CDF of  $Z_{\text{RIS}}$  can be expressed as

$$F_{Z_{\text{RIS}}}(x) \leq F_{Y_{\text{RIS}}}\left(\left(\frac{x}{N}\right)^N\right) \quad (18)$$

where  $Y_{\text{RIS}} = \prod_{i=1}^N Z_i$  is the product of  $Z_i$  with  $i = 1, 2, 3, \dots, N$ . Similarly, an upper bound on the PDF of  $Z_{\text{RIS}}$  is:

$$f_{Z_{\text{RIS}}}(x) \leq \left(\frac{x}{N}\right)^{N-1} f_{Y_{\text{RIS}}}\left(\left(\frac{x}{N}\right)^N\right) \quad (19)$$

It can be seen from (18) and (19) that statistical results of  $Z_{\text{RIS}}$  requires the PDF and CDF of  $N$ -product of  $Z_i$ . We can use the Mellin inverse transform to get the PDF of  $Y_{\text{RIS}} = \prod_{i=1}^N Z_i$  [13], [33]:

$$f_{Y_{\text{RIS}}}(x) = \frac{x^{-1}}{2\pi j} \int_{\mathcal{L}} \mathbb{E}[Y_{\text{RIS}}^r] x^{-r} dr = \frac{x^{-1}}{2\pi j} \int_{\mathcal{L}} \prod_{i=1}^N \mathbb{E}[(Z_i)^r] x^{-r} dr \quad (20)$$

where  $\mathbb{E}[\cdot]$  denotes the expectation operator.

**Lemma 2.** *Upper bounds on the PDF and CDF of the resultant RIS channel  $Z_{\text{RIS}}$  are given by*

$$f_{Z_{\text{RIS}}}(x) \leq \left(\frac{x}{N}\right)^{-1} \sum_{k_1, \dots, k_N=0}^{\infty} \sum_{j_1, \dots, j_N=1}^n \prod_{i=1}^N \psi_i H_{N+1,4N+1}^{3N,N} \left[ \prod_{i=1}^N \zeta_{i,1} \zeta_{i,2} \left(\frac{x}{N}\right)^N \mid \left\{ (-\beta_{j_i}, \frac{a}{2}) \right\}_1^N, (1, q) \right] \quad (21)$$

$$F_{Z_{\text{RIS}}}(x) \leq \sum_{k_1, \dots, k_N=0}^{\infty} \sum_{j_1, \dots, j_N=1}^n \prod_{i=1}^N \psi_i H_{N+2,4N+2}^{3N,N+1} \left[ \prod_{i=1}^N \zeta_{i,1} \zeta_{i,2} \left(\frac{x}{N}\right)^N \mid \left\{ (-\beta_{j_i}, \frac{a}{2}) \right\}_1^N, (1, 1), (1, q) \right] \quad (22)$$

where  $V_i = (\beta_{i,2}, \frac{1}{\alpha_{i,2}}), (\beta_{i,1}, \frac{1}{\alpha_{i,1}}), (\mu_i + k_i, 1), (-1 - \beta_{j_i}, \frac{a}{2})$ .

*Proof:* See Appendix C. ■

As a special case, we can use the proof of Appendix C with (10) for Rayleigh fading channels with phase noise and mobility to get upper bounds on the PDF and CDF of  $Z_{\text{RIS}}$ :

$$f_{Z_{\text{RIS}}}(x) \leq \left(\frac{x}{N}\right)^{-1} \sum_{j_1, \dots, j_N=1}^n \prod_{i=1}^N B_{j_i} H_{N+1,3N+1}^{2N,N} \left[ \prod_{i=1}^N \frac{2}{\Omega_{i,1}} d_2^{\frac{a}{2}} \left(\frac{x}{N}\right)^N \mid \left\{ (-\beta_{j_i}, \frac{a}{2}) \right\}_1^N, (1, q) \right] \quad (23)$$

$$F_{Z_{\text{RIS}}}(x) \leq \sum_{j_1, \dots, j_N=1}^n \prod_{i=1}^N B_{j_i} H_{N+2,3N+2}^{2N,N+1} \left[ \prod_{i=1}^N \frac{2}{\Omega_{i,1}} d_2^{\frac{a}{2}} \left(\frac{x}{N}\right)^N \mid \left\{ (-\beta_{j_i}, \frac{a}{2}) \right\}_1^N, (1, 1), (1, q) \right] \quad (24)$$

where  $V_i = (2, 1), (1, 1), (-1 - \beta_{j_i}, \frac{a}{2})$ . Similarly, upper bounds for the PDF and CDF of  $Z_{\text{RIS}}$  for Rayleigh fading channels with phase noise can be derived as

$$f_{Z_{\text{RIS}}}(x) \leq \left(\frac{x}{N}\right)^{-1} H_{N+1,3N+1}^{2N,N} \left[ \prod_{i=1}^N \frac{2}{\Omega_{i,1}} \left(\frac{x}{N}\right)^N \mid \left\{ (2, 1), (1, 1) \right\}_1^N, (0, q) \right] \quad (25)$$

$$F_{Z_{\text{RIS}}}(x) \leq H_{N+2,3N+2}^{2N,N+1} \left[ \prod_{i=1}^N \frac{2}{\Omega_{i,1}} \left(\frac{x}{N}\right)^N \mid \left\{ (2, 1), (1, 1) \right\}_1^N, (0, 1), (0, q) \right] \quad (26)$$

where  $V_i = (2, 1), (1, 1), (-1 - \beta_{j_i}, \frac{a}{2})$ .

### B. With Direct Link ( $\omega = 1$ )

In this subsection, we provide statistical results for the considered RIS-assisted system with direct link by applying the maximal ratio combining (MRC) receiver at the destination for the received signals from the RIS and direct transmissions. Here, we develop statistical results for the resultant SNR of the RIS-assisted system given as  $\gamma_{\text{RISD}} = \gamma_{\text{RIS}} + \gamma_d = \bar{\gamma}_{\text{RIS}} Z_{\text{RIS}}^2 + \bar{\gamma}_d Z_d^2$ , where  $\bar{\gamma}_{\text{RIS}} = \frac{H_t^2 P_t}{\sigma^2}$  and  $\bar{\gamma}_d = \frac{P_t}{\sigma^2}$ .

The PDF and CDF of SNR of RIS link  $f_{\gamma_{\text{RIS}}}(\gamma)$  can be expressed using mathematical transformation as

$$f_{\gamma_{\text{RIS}}}(\gamma) = \frac{1}{2\sqrt{\gamma_{\text{RIS}}\gamma}} f_{Z_{\text{RIS}}}(\sqrt{\frac{\gamma}{\gamma_{\text{RIS}}}}) \quad (27)$$

$$F_{\gamma_{\text{RIS}}}(\gamma) = F_{Z_{\text{RIS}}}(\sqrt{\frac{\gamma}{\gamma_{\text{RIS}}}}) \quad (28)$$

We denote the direct link path gain component as  $h_{l,d}^{\text{rwp}} = r^{-\frac{\alpha}{2}}$ , where  $r$  is random due to the mobility of user. Thus, the PDF of short-term fading of the direct link combined with mobility model can be expressed as

$$f_{Z_d}(x) = \int_0^d f_{Z_d}(x/r) f_r(r) dr \quad (29)$$

Applying standard mathematical procedure, the PDF of the SNR  $\bar{\gamma}_d Z_d^2$  for the direct-link channel combined with mobility model is given as

$$f_{\gamma_d}(x) = \sum_{j=1}^n \psi_d x^{M+m-1} H_{0,3}^{2,1} \left[ \frac{bd\frac{\alpha}{2}x}{2} \mid \left(\frac{M-m}{2}, \frac{1}{2}\right), \left(\frac{m-M}{2}, \frac{1}{2}\right), \left(\beta_j + \frac{a(M+m)}{2}, \frac{a}{2}\right), \left(\beta_j + \frac{a(M+m)}{2} + 1, \frac{a}{2}\right) \right] \quad (30)$$

where  $\psi_d = B_j \frac{b^{M+m} d^{\frac{a(M+m)}{2}}}{2^{M+m} \Gamma(m) \Gamma(M)}$ .

To derive the PDF of  $\gamma_{\text{RISD}} = \gamma_{\text{RIS}} + \gamma_d$ , we first compute the MGF of  $\gamma_{\text{RIS}}$  and  $\gamma_d$  and apply the inverse Laplace transform, as presented in the following Theorem:

**Theorem 2.** *Exact and upper bounds for the PDF and CDF of the resultant SNR  $\gamma_{\text{RISD}} = \gamma_{\text{RIS}} + \gamma_d$  are given in (31) and (32).*

*Proof:* Refer to Appendix D. ■

In the following section, we use the derived statistical results to analysis the performance of RIS-assisted system with/without direct link under the combined effect of phase noise and mobility.

#### IV. PERFORMANCE ANALYSIS

In this section we analyze the outage probability and average BER of RIS system without and with direct link. We derive exact expressions, upper bound and asymptotic expressions at high SNR for the considered systems.

To analyze the system performance, we use the CDF of the SNR presented in the previous section. For the case without direct link  $\omega = 0$ , the CDF of the SNR  $\gamma_{\text{RIS}}$  is  $F_{\gamma_{\text{RIS}}}(\gamma) = F_{Z_{\text{RIS}}}(\sqrt{\frac{\gamma}{\gamma_{\text{RIS}}}})$ , where  $F_{Z_{\text{RIS}}}(x)$  is derived in Section III-A for various scenarios. Similarly, the CDF of the SNR with direct link (i.e.,  $\omega = 1$ )  $F_{\gamma_{\text{RISD}}}(\gamma)$  is derived in Section III-B.

##### A. Outage Probability

Outage probability is a performance metric to characterize the impact of fading in a communication system. Mathematically, it can be defined as the probability of SNR falling below a threshold value  $\gamma_{\text{th}}$  i.e.,  $P_{\text{out}} = Pr(\gamma \leq \gamma_{\text{th}})$ . Thus, an exact expression for the RIS system can be expressed as  $F_{\gamma_{\text{RIS}}}(\gamma_{\text{th}})$  for without direct link and  $F_{\gamma_{\text{RISD}}}(\gamma_{\text{th}})$  with direct link.

To get the outage probability at a high SNR, we can apply the asymptotic series expansion [39], [40] on the CDF functions represented in terms of  $N$ -multivariate (exact expression

without direct link (13)),  $N+1$ -multivariate (exact expression with direct link (32)), univariate (upper bound without direct link (22)), bivariate (upper bound with direct link (32)) Fox's H-function.

To illustrate, we apply [40, eq. (30)] on the  $N+1$ -multivariate Fox's H-function in (32), to represent the outage probability asymptotically at a high SNR regime for the RIS-assisted system with direct link:

$$P_{\text{out,RISD}}^{\infty} = \frac{1}{4} \sum_{k_1, \dots, k_N=0}^{\infty} \sum_{j_1, \dots, j_N=1}^n \sum_{j=1}^n \prod_{i=1}^N B_j \psi_i \frac{1}{\Gamma(m)\Gamma(M)} \frac{\Gamma(\frac{p_1}{2} + \dots + \frac{p_N}{2})}{\Gamma(p_1 + \dots + p_N) \Gamma(1 + \frac{p_1}{2} + \dots + \frac{p_N}{2} + \frac{p_N + p_N + 1}{2})} \prod_{i=1}^N \frac{\Gamma(\beta_{i,2} - \frac{p_i}{\alpha_{i,2}}) \Gamma(\beta_{i,1} - \frac{p_i}{\alpha_{i,1}}) \Gamma(\mu_i + k_i - p_i) \Gamma(1 + \beta_{j_i} + \frac{\alpha_{p_i}}{2}) \Gamma(p_i)}{\Gamma(2 + \beta_{j_i} + \frac{\alpha_{p_i}}{2}) \Gamma(1 - qp_i) \Gamma(1 + qp_i)} (\zeta_{i,1} \zeta_{i,2} \sqrt{\frac{\gamma_{\text{th}}}{\gamma_{\text{RIS}}}})^{p_i - 1} \frac{\Gamma(M - \frac{p_N + 1}{2}) \Gamma(m - \frac{p_N + 1}{2}) \Gamma(1 - \beta_j + a(M+m) + \frac{\alpha_{p_N + 1}}{2}) \Gamma(\frac{p_N + 1}{2})}{\Gamma(\beta_j + a(M+m) + \frac{\alpha_{p_N + 1}}{2})} (bd\frac{\alpha}{2} \sqrt{\frac{\gamma_{\text{th}}}{\gamma_d}})^{p_{N+1} - 1} \quad (33)$$

where  $p_i = \min\{\alpha_{i,1}\beta_{i,1}, \alpha_{i,2}\beta_{i,2}, \mu_i\}$  for  $i \in (1, N)$ ,  $p_{N+1} = \min\{2M, 2m\}$  is the dominant term.

To get the outage diversity order of the system, we can express (33) as  $P_{\text{out,RISD}}^{\infty} \propto \bar{\gamma}^{-G_{\text{out}}}$  resulting  $G_{\text{out}} = \sum_{i=1}^{N+1} \frac{p_i}{2}$ . Thus, the diversity order provides various design criteria depending on the fading and system parameters. It can be seen that diversity order is independent of the parameter  $\kappa$ .

##### B. Average BER

Average BER is used to quantify the reliability of data transmissions. For binary modulations, the average BER using the CDF of SNR is given as [41]

$$\bar{P}_e = \frac{q^p}{2\Gamma(p)} \int_0^{\infty} \gamma^{p-1} e^{-q\gamma} F_{\gamma}(\gamma) d\gamma \quad (34)$$

where  $p$  and  $q$  are modulation specific parameters.

For the RIS-assisted system with direct link ( $\omega = 1$ ), we substitute the exact expression of the CDF (see (32)) in (34) and expand the definition of multivariate Fox-H function and interchange the order of integration to get

$$\bar{P}_{e,\text{RISD}} = \frac{q^p}{2\Gamma(p)} \sum_{k_1, \dots, k_N=0}^{\infty} \sum_{j_1, \dots, j_N=1}^n \sum_{j=1}^n \prod_{i=1}^N B_j \psi_i \frac{1}{\Gamma(m)\Gamma(M)} \frac{1}{2\pi j} \int_{\mathcal{L}_i} (\zeta_{i,2} \zeta_{i,1} \sqrt{\frac{1}{\gamma_{\text{RIS}}}})^{s_i} \frac{\Gamma(1 + \beta_{j_i} + \frac{\alpha}{2} s_i) \Gamma(\beta_{i,1} - \frac{s_i}{\alpha_{i,1}}) \Gamma(\beta_{i,2} - \frac{s_i}{\alpha_{i,2}}) \Gamma(\mu_i + k_i - s_i) \Gamma(s_i)}{\Gamma(2 + \beta_{j_i} + \frac{\alpha}{2} s_i) \Gamma(1 - qs_i) \Gamma(1 + qs_i)} \frac{\Gamma(\sum_{i=1}^N \frac{s_i}{2})}{\Gamma(\sum_{i=1}^N s_i)} \frac{1}{2\pi j} \int_{\mathcal{L}_d} (bd\frac{\alpha}{2} \sqrt{\frac{1}{\gamma_d}})^{s_d} \Gamma(\frac{s_d}{2}) \frac{\Gamma(M - \frac{s_d}{2}) \Gamma(m - \frac{s_d}{2}) \Gamma(1 - \beta_j - a(M+m) + \frac{\alpha}{2} s_d)}{\Gamma(-\beta_j - a(M+m) + \frac{\alpha}{2} s_d) \Gamma(\sum_{i=1}^N \frac{s_i}{2} + \frac{s_d}{2} + 1)} \left( \int_0^{\infty} \gamma^{p-1} e^{-q\gamma} \gamma^{\sum_{i=1}^N \frac{s_i}{2} + \frac{s_d}{2}} d\gamma \right) ds_i ds_d \quad (35)$$

Now, the inner integral is solved as  $I = \int_0^{\infty} \gamma^{p-1} e^{-q\gamma} \gamma^{\sum_{i=1}^N \frac{s_i}{2} + \frac{s_d}{2}} d\gamma = (\frac{1}{q})^{p + \sum_{i=1}^N \frac{s_i}{2} + \frac{s_d}{2}} \Gamma(p + \sum_{i=1}^N \frac{s_i}{2} + \frac{s_d}{2})$ . We substitute it back and apply the definition of multivariate Fox's H-function to get an exact expression of the average BER (36). Using the upper bound of the CDF (see (32)) in (34), apply the definition of bi-variate Fox's H-function to get (37).

$$\begin{aligned}
f_{\gamma_{\text{RISD}}}(\gamma) &= \frac{1}{4\gamma} \sum_{k_1, \dots, k_N=0}^{\infty} \sum_{j_1, \dots, j_N=1}^n \sum_{j=1}^n \prod_{i=1}^N B_j \psi_i \frac{1}{\Gamma(m)\Gamma(M)} \\
& H_{1,2:3,5;\dots;3,5:2,2}^{0,1:3,2;\dots;3,2:2,2} \left[ \left\{ \zeta_{i,1} \zeta_{i,2} \sqrt{\frac{\gamma}{\gamma_{\text{RIS}}}} \right\}_1^N \mid (1 : \frac{1}{2}, \dots, \frac{1}{2}, 0) : V_1 \right. \\
& \quad \left. \left( 1 : 1, \dots, 1, 0 \right), (1 : \frac{1}{2}, \dots, \frac{1}{2}, \frac{1}{2}) : V_2 \right] \\
& \leq \frac{N}{4\gamma} \sum_{k_1, \dots, k_N=0}^{\infty} \sum_{j_1, \dots, j_N=1}^n \sum_{j=1}^n \prod_{i=1}^N \psi_i \frac{B_j}{\Gamma(m)\Gamma(M)} \\
& H_{0,1:N+1,4N+1;2,3}^{0,0:3N,N;2,2} \left[ \prod_{i=1}^N \zeta_{i,1} \zeta_{i,2} \left( \frac{1}{N} \sqrt{\frac{\gamma}{\gamma_{\text{RIS}}}} \right)^N \mid - : \{(-\beta_{j_i}, \frac{a}{2})\}_1^N, (1, q); (\beta_j + a(M+m), \frac{a}{2}), (1, \frac{1}{2}) \right. \\
& \quad \left. (1 : \frac{N}{2}, \frac{1}{2}) : V_3, (0, q); (M, \frac{1}{2}), (m, \frac{1}{2}), (1 + \beta_j + a(M+m), \frac{a}{2}) \right] \tag{31}
\end{aligned}$$

$$\begin{aligned}
F_{\gamma_{\text{RISD}}}(\gamma) &= \frac{1}{4} \sum_{k_1, \dots, k_N=0}^{\infty} \sum_{j_1, \dots, j_N=1}^n \sum_{j=1}^n \prod_{i=1}^N B_j \psi_i \frac{1}{\Gamma(m)\Gamma(M)} \\
& H_{1,2:3,5;\dots;3,5:2,2}^{0,1:3,2;\dots;3,2:2,2} \left[ \left\{ \zeta_{i,1} \zeta_{i,2} \sqrt{\frac{\gamma}{\gamma_{\text{RIS}}}} \right\}_1^N \mid (1 : \frac{1}{2}, \dots, \frac{1}{2}, 0) : V_1 \right. \\
& \quad \left. (1 : 1, \dots, 1, 0), (0 : \frac{1}{2}, \dots, \frac{1}{2}, \frac{1}{2}) : V_2 \right] \\
& \leq \frac{N}{4} \sum_{k_1, \dots, k_N=0}^{\infty} \sum_{j_1, \dots, j_N=1}^n \sum_{j=1}^n \prod_{i=1}^N \psi_i \frac{B_j}{\Gamma(m)\Gamma(M)} \\
& H_{0,1:N+1,4N+1;2,3}^{0,0:3N,N;2,2} \left[ \prod_{i=1}^N \zeta_{i,1} \zeta_{i,2} \left( \frac{1}{N} \sqrt{\frac{\gamma}{\gamma_{\text{RIS}}}} \right)^N \mid - : \{(-\beta_{j_i}, \frac{a}{2})\}_1^N, (1, q); (\beta_j + a(M+m), \frac{a}{2}), (1, \frac{1}{2}) \right. \\
& \quad \left. (0 : \frac{N}{2}, \frac{1}{2}) : V_3, (0, q); (M, \frac{1}{2}), (m, \frac{1}{2}), (1 + \beta_j + a(M+m), \frac{a}{2}) \right] \tag{32}
\end{aligned}$$

where  $V_1 = \{(-\beta_{j_i}, \frac{a}{2}), (1, q), (1, 1)\}_{i=1}^N; (\beta_j + a(M+m), \frac{a}{2}), (1, \frac{1}{2})$ ,  $V_2 = \{(\beta_{i,2}, \frac{1}{\alpha_{i,2}}), (\beta_{i,1}, \frac{1}{\alpha_{i,1}}), (\mu_i + k_i, 1), (-1 - \beta_{j_i}, \frac{a}{2}), (0, q)\}_{i=1}^N; (M, \frac{1}{2}), (m, \frac{1}{2}), (1 + \beta_j + a(M+m), \frac{a}{2})$ , and  $V_3 = \{(\beta_{i,2}, \frac{1}{\alpha_{i,2}}), (\beta_{i,1}, \frac{1}{\alpha_{i,1}}), (\mu_i + k_i, 1), (-1 - \beta_{j_i}, \frac{a}{2})\}_1^N$ .

$$\begin{aligned}
\bar{P}_{e,\text{RISD}} &= \frac{1}{8\Gamma(p)} \sum_{k_1, \dots, k_N=0}^{\infty} \sum_{j_1, \dots, j_N=1}^n \sum_{j=1}^n \prod_{i=1}^N B_j \psi_i \frac{1}{\Gamma(m)\Gamma(M)} \\
& H_{2,2:3,5;\dots;3,5:2,2}^{0,2:3,2;\dots;3,2:2,2} \left[ \left\{ \zeta_{i,1} \zeta_{i,2} \sqrt{\frac{1}{q\gamma_{\text{RIS}}}} \right\}_1^N \mid (1 : \frac{1}{2}, \dots, \frac{1}{2}, 0), (1 - p : \frac{1}{2}, \dots, \frac{1}{2}, \frac{1}{2}) : V_1 \right. \\
& \quad \left. (1 : 1, \dots, 1, 0), (0 : \frac{1}{2}, \dots, \frac{1}{2}, \frac{1}{2}) : V_2 \right] \tag{36} \\
& \leq \frac{N}{8\Gamma(p)} \sum_{k_1, \dots, k_N=0}^{\infty} \sum_{j_1, \dots, j_N=1}^n \sum_{j=1}^n \prod_{i=1}^N \psi_i \frac{B_j}{\Gamma(m)\Gamma(M)} \\
& H_{1,1:N+1,4N+1;2,3}^{0,1:3N,N;2,2} \left[ \prod_{i=1}^N \zeta_{i,1} \zeta_{i,2} \left( \frac{1}{N} \sqrt{\frac{1}{q\gamma_{\text{RIS}}}} \right)^N \mid (1 - p : \frac{N}{2}, \frac{1}{2}) : V_3 \right. \\
& \quad \left. (0 : \frac{N}{2}, \frac{1}{2}) : V_4 \right] \tag{37}
\end{aligned}$$

where  $V_1 = \{(-\beta_{j_i}, \frac{a}{2}), (1, q), (1, 1)\}_{i=1}^N; (\beta_j + a(M+m), \frac{a}{2}), (1, \frac{1}{2})$ ,  $V_2 = \{(\beta_{i,2}, \frac{1}{\alpha_{i,2}}), (\beta_{i,1}, \frac{1}{\alpha_{i,1}}), (\mu_i + k_i, 1), (-1 - \beta_{j_i}, \frac{a}{2}), (0, q)\}_{i=1}^N; (M, \frac{1}{2}), (m, \frac{1}{2}), (1 + \beta_j + a(M+m), \frac{a}{2})$ ,  $V_3 = \{(-\beta_{j_i}, \frac{a}{2})\}_1^N, (1, q); (\beta_j + a(M+m), \frac{a}{2}), (1, \frac{1}{2})$ , and  $V_4 = \{(\beta_{i,2}, \frac{1}{\alpha_{i,2}}), (\beta_{i,1}, \frac{1}{\alpha_{i,1}}), (\mu_i + k_i, 1), (-1 - \beta_{j_i}, \frac{a}{2})\}_1^N, (0, q); (M, \frac{1}{2}), (m, \frac{1}{2}), (1 + \beta_j + a(M+m), \frac{a}{2})$ .

Similar to the direct link scenario, we can develop results for without direct link, as given by (38) and (39), respectively.

## V. SIMULATION AND NUMERICAL RESULTS

In this section, we use numerical analysis and Monte Carlo simulations (averaged over  $10^8$  channel realizations) to demonstrate the effect of phase noise and mobility on the performance of RIS-assisted transmission over generalized fading channels. We also validate the derived analytical expressions and bounds using simulations. For numerical computation, we use Python code implementation of multivariable Fox's H-function [38]. To demonstrate the effect of phase noise and mobility, we also plot the performance of RIS-assisted system with perfect phase compensation and no mobility for reference. To compute the path loss component of the RIS without mobility, we assume that the user is placed at the half of the distance  $\frac{d_2}{2}$ , and for the moving destination, we use the RWP model, as described in the system model section.

We consider carrier frequency  $f = 6\text{GHz}$ , transmit antenna gain  $G_T = 10\text{dBi}$ , and receive antenna gain  $G_R = 10\text{dBi}$ . We assume the RIS situated perpendicular to the source and destination with a distance from the source to RIS at  $d_1 = 50\text{m}$  and the RIS to destination at  $d_2 = 100\text{m}$  such that direct transmission distance from the source to the destination  $d_d = \sqrt{d_1^2 + d_2^2} = 111.8\text{ m}$ . A noise floor of  $-74\text{dBm}$  is considered over a  $20\text{MHz}$  channel bandwidth. For simulations, we assume i.i.d. channel fading coefficients from the source to all RIS elements and similarly from all RIS elements to the destination. Channel parameters used in the simulations are as follows: for the first link ( $\kappa$ - $\mu$  fading), we take  $\kappa_i = 4$ ,  $\mu_i = 2$ , and for the second link (dGG fading), we take  $\alpha_{i,1} = \alpha_1 = 2$ ,  $\beta_{i,1} = \beta_1 = 1$ ,  $\alpha_{i,2} = \alpha_2 = 2$  and  $\beta_{i,1} = \beta_2 = 2 \forall i$ . To model the phase noise, we consider two quantization levels  $L = 1$  and  $l2$ , and assume different mobility models with varying path loss exponent factor  $2 \leq a \leq 5$  to demonstrate the effect of mobility on the systems performance.

### A. Effect of Phase Noise and Mobility without Direct Link $\omega = 0$ (See Fig. 2, Fig. 3, Fig. 4, and Fig. 5)

We demonstrate the outage probability and average BER considering a phase noise level  $L = 1$  (1-bit quantization) for different mobility scenarios and path loss exponent  $a$ , as shown in Fig. 2 and Fig. 3, respectively. Fig. 2 shows the outage probability of RIS-assisted system for different mobility models with and without phase errors. We have also plotted the outage probability for the case when destination is not moving and is situated at the mid-way. Fig. 2 shows that there is a difference in performance considering the case of with and without RWP model. The use of mobility model can provide a more realistic performance estimate than the static case in the context of vehicular communications. Further, there is difference of  $1\text{dBm}$  and  $2\text{dBm}$  in transmit power to achieve the same outage probability for 1-D and 3-D models, respectively. Fig. 2 also depicts the impact of imperfect phase compensation represented by 1-bit quantization at RIS: a significant  $6\text{dBm}$  higher transmit power is required

to achieve a desired outage performance of  $10^{-3}$  compared with the optimal phase compensating system. We also show the significance of adding RIS elements  $N$ , which shows a significant scaling of the outage performance for the RIS-assisted system.

Fig. 3 shows the average BER of the RIS system for varying path loss exponent for  $N = 10$ ,  $L = 1$  and 1-D RWP model. Here, BER performance degrades with an increase in the path loss exponent  $a$  from 2 to 2.5 and then to 3, as expected. We can observe about  $8\text{dBm}$  loss in system performance when  $a$  is changed from 2 to 2.5 and then 2.5 to 3. We have also plotted RIS performance with phase errors but without effect mobility demonstrating the gap in the performance with an increase in the parameter  $a$ .

In Fig. 4 and Fig. 5, we demonstrate the impact of imperfect phase on the RIS-assisted system performance considering a fixed RWP mobility model (1-D) with a path loss exponent  $a = 2$ . We plot the outage probability and average BER for different phase noise quantization levels  $L = 1$ ,  $L = 2$  for various number of reflecting elements  $N$  of the RIS module, as shown in Fig. 4 and Fig. 5, respectively. We compare the performance with an optimal criteria assuming perfect phase compensation. The figure shows that the performance for moving user is slightly better than the static user by comparing the optimal performance with 1-D mobility plots since the user can be near to the RIS using the RWP model compared to static user assumed to be situated at the midpoint. Further, Fig. 4 shows performance degradation in the presence of phase noise. It can be seen that a loss of  $5\text{dBm}$  transmit power with 1-bit quantization compared to  $L = 2$  to achieve an outage performance of  $10^{-3}$ . However, the effect of phase noise can be compensated by increasing the quantization level  $L$  or by increasing the number of RIS elements  $N$ . Thus, the outage probability and average BER with a higher phase noise quantization level  $L = 2$  or doubling  $N$  at the fixed level  $L = 1$  achieves a near-optimal performance. It appears that higher order quantization steps can mitigate the effect of phase noise with higher complexity at the RIS, which is not desirable for RIS deployment. However, the figures show that an increase in RIS elements  $N$  can provide optimal even at a lower quantization level  $L = 1$  with large RIS size. For example, an average BER performance of  $10^{-4}$  can be achieved with  $N = 10$ ,  $L = 2$  at  $38\text{dBm}$  of transmit power. The same performance can be achieved with higher  $N = 20$  at a lower quantization  $L = 1$  at a transmit power of  $34\text{dBm}$ . Further, a higher  $N = 50$  with  $L = 1$  require  $24\text{dBm}$  of transmit power to achieve an average BER performance of  $10^{-4}$ . Thus, a large-size RIS can provide near-optimal in the presence of phase noise.

In all the above figures, we also validate the derived analytical results by comparing numerical computations obtained from exact analytical expressions with Monte-Carlo simulations. Further, we have also plotted upper bound in Fig. 4 and Fig. 5. The figure shows that exact analysis has an excellent agreement with simulations but there is a difference between the exact and the upper bound due to the use of arithmetic and geometric mean inequality. Further, slope of simulation plots depict that the diversity order of system is independent



$$\bar{P}_{e,\text{RIS}} = \frac{1}{8\Gamma(p)} \sum_{k_1, \dots, k_N=0}^{\infty} \sum_{j_1, \dots, j_N=1}^n \prod_{i=1}^N \psi_i$$

$$H_{2,2;2:3,2;\dots;3,2}^{0,2:3,2;\dots;3,2} \left[ \{\zeta_{i,1}\zeta_{i,2}\sqrt{\frac{1}{q\gamma_{\text{RIS}}}}\}_1^N \mid \begin{matrix} (1:\frac{1}{2}, \dots, \frac{1}{2}), (1-p:\frac{1}{2}, \dots, \frac{1}{2}): V_1 \\ (1:1, \dots, 1), (0:\frac{1}{2}, \dots, \frac{1}{2}): V_2 \end{matrix} \right] \quad (38)$$

$$\leq \frac{N}{8\Gamma(p)} \sum_{k_1, \dots, k_N=0}^{\infty} \sum_{j_1, \dots, j_N=1}^n \prod_{i=1}^N \psi_i$$

$$H_{1,1:1:3N,N}^{0,1:3N,N} \left[ \prod_{i=1}^N \zeta_{i,1}\zeta_{i,2} \left(\frac{1}{N}\sqrt{\frac{1}{q\gamma_{\text{RIS}}}}\right)^N \mid \begin{matrix} (1-p:\frac{N}{2}): V_3 \\ (0:\frac{N}{2}): V_4 \end{matrix} \right] \quad (39)$$

where  $V_1 = \{(-\beta_{j_i}, \frac{a}{2}), (1, q), (1, 1)\}_{i=1}^N$ ,  $V_2 = \{(\beta_{i,2}, \frac{1}{\alpha_{i,2}}), (\beta_{i,1}, \frac{1}{\alpha_{i,1}}), (\mu_i + k_i, 1), (-1 - \beta_{j_i}, \frac{a}{2}), (0, q)\}_{i=1}^N$ ,  $V_3 = \{(-\beta_{j_i}, \frac{a}{2})\}_1^N, (1, q)$ , and  $V_4 = \{(\beta_{i,2}, \frac{1}{\alpha_{i,2}}), (\beta_{i,1}, \frac{1}{\alpha_{i,1}}), (\mu_i + k_i, 1), (-1 - \beta_{j_i}, \frac{a}{2})\}_1^N, (0, q)$ .

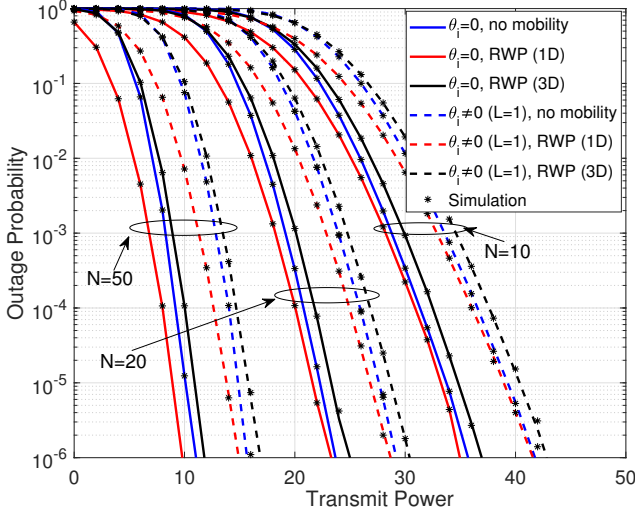


Fig. 2. Outage performance of the RIS-assisted system without direct link ( $\omega = 0$ ) for phase noise level  $L = 1$  at different mobility parameters.

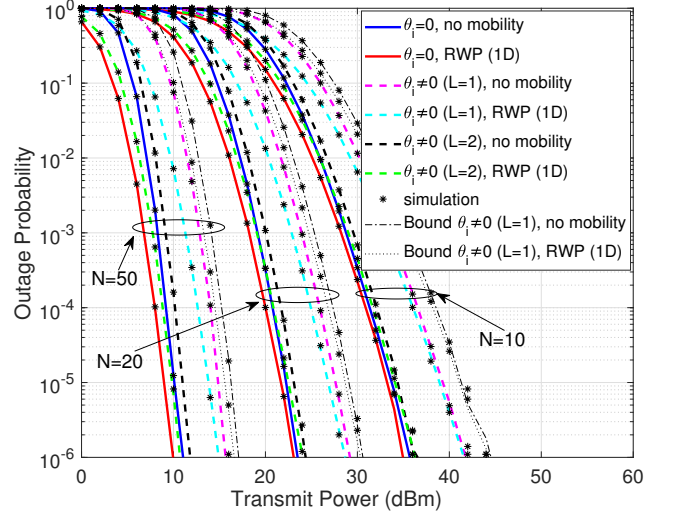


Fig. 4. Outage performance of RIS-assisted system without direct link ( $\omega = 0$ ) with 1-D mobility at different phase noise parameters.

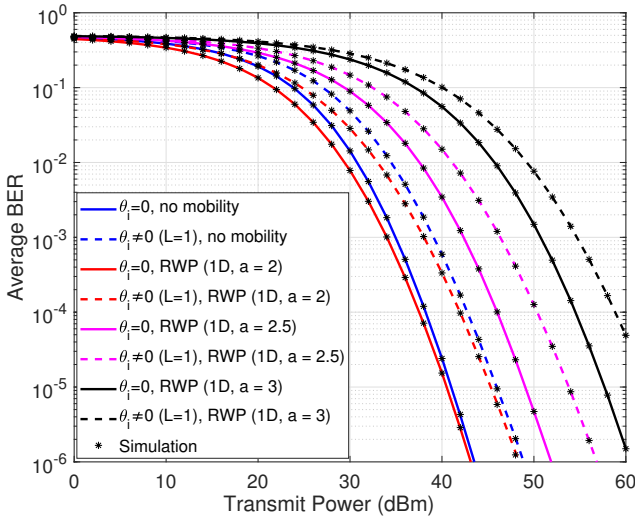


Fig. 3. Average BER of the RIS-assisted system without direct link ( $\omega = 0$ ) for phase noise level  $L = 1$  at different mobility parameters.

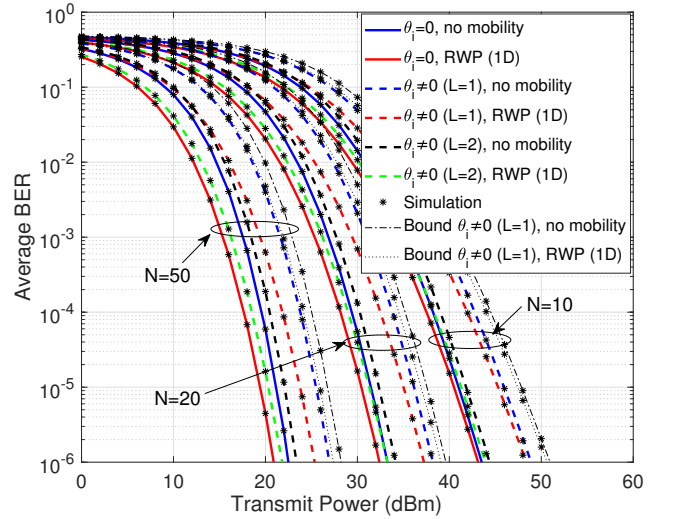


Fig. 5. Average BER of RIS-assisted system without direct link ( $\omega = 0$ ) with 1-D mobility at different phase noise parameters.

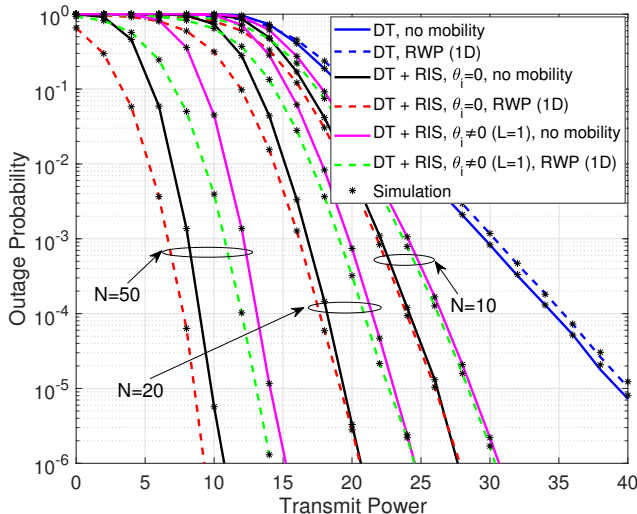


Fig. 6. Outage Performance of RIS-assisted system with direct link ( $\omega = 1$ ) for different phase noise levels and varying mobility parameters.

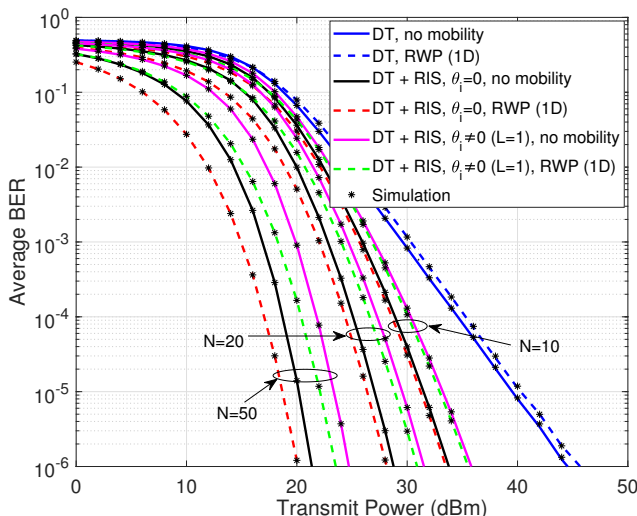


Fig. 7. Effect of phase noise and varying mobility parameters on average BER of RIS-assisted system with direct link ( $\omega = 1$ ).

of mobility and phase errors, which can be useful for adapting the system and channel parameters for optimized performance.

### B. Effect of Phase Noise and Mobility with Direct Link $\omega = 1$ (See Fig. 6 and Fig. 7)

In this section, we demonstrate the performance of RIS-assisted with direct link  $\omega = 1$ . For the direct link, we use the generalized- $\mathcal{K}$  shadowing fading model with  $m = 1$ ,  $\sigma_{dB} = 4\text{dB}$  and  $M = 2.5454$ . The outage and average BER performance of the RIS-assisted system combined with direct link are shown in Fig. 6 and Fig. 7, respectively. It is clear from the plots that the combined system with direct link performs better than individual systems (direct link only and RIS-assisted without direct link  $\omega = 0$ ) for a wider range of SNR. It can be seen that the direct transmission (DT) performs

better at low transmit powers compared with a smaller  $N$  RIS. However, RIS-assisted transmission (without direct link) outperforms DT for a reasonable  $N$ . Fig. 7 also demonstrates that the average BER performance of the combined system is significantly better than the direct transmission at a high transmit power by harnessing the line-of-sight signal from the RIS elements. Moreover, the performance of RIS combined with direct transmission is always better than the RIS system (without DT) even at low SNR. For instance, we can observe a gain in transmit power of about 8dBm for  $N = 10$  and 14dBm for  $N = 20$  to achieve a desired outage performance of  $10^{-3}$  compared to the DT. Hence, it is clear that combined system performance is better than individual systems thereby exploiting the presence of DT at low SNRs and the LOS signal received through RIS at high SNRs. further, in the presence of direct link, phase errors represented by lower quantization  $L$  can be undone with proportionately lesser  $N$  compared to RIS-assisted system without direct link.

## VI. CONCLUSIONS

We developed exact analysis and upper bounds on the performance of RIS-assisted vehicular communication system considering phase noise with mobility over asymmetric fading channels by coherently combining received signals reflected by RIS elements and direct transmissions from the source terminal. We adopted the generalized uniform distribution to model the phase noise, the RWP model for mobility, generalized- $\mathcal{K}$  shadowed fading distribution for the direct link. We presented outage and average BER performance of the considered system in terms of univariate and multivariate Fox's  $H$  functions. We also derived simplified expressions at high SNR in terms of gamma functions to compute the diversity order of the system. We used computer simulations to demonstrate the effect of phase noise and mobility on the RIS-assisted performance compared with the optimal performance with perfect phase compensation. For RIS-assisted vehicular network, consideration of a statistical model for mobility provides a better estimate on the performance. Further, the effect of phase noise can be mitigated by increasing the number of elements in the RIS module and using higher quantization level for the phase error. Further, our analysis demonstrates the effectiveness of the coherent combining of reflected signals from RIS and the signal from direct link to achieve reliable performance even with phase noise and user under movement.

It would be interesting to analyze the system performance considering a measurement based mobility model and correlated fading channels in the presence of phase noise.

### APPENDIX A: PDF OF SINGLE-ELEMENT RIS WITH USER MOBILITY AND PHASE ERRORS $Z_i$

To compute the PDF of  $Z_i$  for the product of four random variable as  $Z_i = |h_i^{(f)}|g_{l,i}^{\text{rwp}}|g_i^{(f)}|e^{j\theta_i}$ , we first derive the PDF of second link with mobility  $g_i = g_{l,i}^{\text{rwp}}|g_i^{(f)}|$ , then combine with the first link to get PDF of  $Z_{hg,i} = h_i g_i$ , and finally apply a novel approach to derive the PDF  $Z_i = Z_{hg,i}e^{j\theta_i}$ .

Assuming a path gain model  $g_{l,i}^{\text{rwp}} = r^{-\frac{\alpha}{2}}$ , the PDF of dGG short-term fading combined with mobility model can be computed as

$$f_{g_i}(x) = \int_0^{d_2} f_{g_i}(x/r) f_r(r) dr \quad (40)$$

where  $f_r(r)$  is the PDF for the RWP model (see (7)). Thus, the PDF of  $f_{g_i}(x/r)$  for a given  $r$  can be expressed as

$$f_{g_i}(x/r) = r^{\frac{\alpha}{2}} f_{|g_i^{(f)}|}(xr^{\frac{\alpha}{2}}) = \frac{1}{\Gamma(\beta_{i,1})\Gamma(\beta_{i,2})} x^{-1} H_{0,2}^{2,0} \left[ \phi_{g,i}^{\frac{1}{\alpha_{i,2}}} r^{\frac{\alpha}{2}} x \mid (\beta_{i,2}, \frac{1}{\alpha_{i,2}}), (\beta_{i,1}, \frac{1}{\alpha_{i,1}}) \right] \quad (41)$$

Substituting (41) in (40) and expanding the definition of Fox's H-function and interchanging the order of integration, we get

$$f_{g_i}(x) = \sum_{j_i=1}^n B_{j_i} \frac{1}{d_2^{\beta_{j_i}+1}} \frac{1}{\Gamma(\beta_{i,1})\Gamma(\beta_{i,2})} x^{-1} \frac{1}{2\pi j} \int_{\mathcal{L}} \phi_{g,i}^{\frac{\alpha}{2}} x^s \Gamma(\beta_{i,2} - \frac{s}{\alpha_{i,2}}) \Gamma(\beta_{i,1} - \frac{s}{\alpha_{i,1}}) \int_0^{d_2} r^{\frac{\alpha s}{2} + \beta_{j_i}} dr ds \quad (42)$$

Invoking the inner integral in (42)

$$\int_0^{d_2} r^{\frac{\alpha s}{2} + \beta_{j_i}} dr = \frac{\Gamma(\frac{\alpha s}{2} + \beta_{j_i} + 1)}{\Gamma(\frac{\alpha s}{2} + \beta_{j_i} + 2)} d_2^{\frac{\alpha s}{2} + \beta_{j_i} + 1} \quad (43)$$

and applying the definition of Fox's H-function, we represent (42)

$$f_{g_i}(x) = \sum_{j_i=1}^n \psi_{i,2} x^{-1} H_{1,3}^{2,1} \left[ \zeta_{i,2} x \mid (\beta_{i,2}, \frac{1}{\alpha_{i,2}}), (\beta_{i,1}, \frac{1}{\alpha_{i,1}}), (-1 - \beta_{j_i}, \frac{\alpha}{2}) \right] \quad (44)$$

where  $\psi_{i,2} = \frac{B_{j_i}}{\Gamma(\beta_{i,1})\Gamma(\beta_{i,2})}$ ,  $\zeta_{i,2} = \phi_{g,i}^{\frac{1}{\alpha_{i,2}}} d_2^{\frac{\alpha}{2}}$ .

Next, PDF of product of two random variables  $Z_{hg,i} = |h_i^{(f)}|g_i$  can be derived as

$$f_{Z_{hg,i}}(x) = \int_0^{\infty} \frac{1}{u} f_{|h_i^{(f)}|}(u) f_{g_i}(\frac{x}{u}) du \quad (45)$$

Substituting (3) and (44) in (45), expanding the definition of Fox's-H function, and interchanging the order of integration, we get

$$f_{Z_{hg,i}}(x) = \sum_{k_i=0}^{\infty} \sum_{j_i=1}^n \psi_{i,1} \psi_{i,2} x^{-1} \frac{1}{2\pi j} \int_{\mathcal{L}_i} (\zeta_{i,2}^{-1} x^{-1})^{s_i} \frac{\Gamma(1+\beta_{j_i} - \frac{\alpha}{2} s_i) \Gamma(\beta_{i,1} + \frac{1}{\alpha_{i,1}} s_i) \Gamma(\beta_{i,2} + \frac{1}{\alpha_{i,2}} s_i)}{\Gamma(2+\beta_{j_i} - \frac{\alpha}{2} s_i)} \int_0^{\infty} u^{s_i + \mu_i + k_i - 1} e^{-\zeta_{i,1} u} du ds_i \quad (46)$$

Solving the inner integral in (46)

$$\begin{aligned} & \int_0^{\infty} u^{s_i + \mu_i + k_i - 1} e^{-\zeta_{i,1} u} du \\ &= \frac{1}{(\zeta_{i,1})^{s_i + \mu_i + k_i}} \int_0^{\infty} u^{s_i + \mu_i + k_i - 1} e^{-u} du \\ &= \frac{1}{(\zeta_{i,1})^{s_i + \mu_i + k_i}} \Gamma(s_i + \mu_i + k_i) \end{aligned} \quad (47)$$

and applying the definition of Fox's-H function, we can express (46) as

$$f_{Z_{hg,i}}(x) = \sum_{k_i=0}^{\infty} \sum_{j_i=1}^n \psi_{i,1} x^{-1} H_{1,4}^{3,1} \left[ \zeta_{i,1} \zeta_{i,2} x \mid \left( -\beta_{j_i}, \frac{\alpha}{2} \right) \right] \quad (48)$$

where  $\psi_{i,1} = \psi_{i,1} \psi_{i,2} \zeta_{i,1}^{-(\mu_i + k_i)}$ ,  $V_i = (\beta_{i,2}, \frac{1}{\alpha_{i,2}}), (\beta_{i,1}, \frac{1}{\alpha_{i,1}}), (\mu_i + k_i, 1), (-1 - \beta_{j_i}, \frac{\alpha}{2})$ .

Finally, we apply a novel approach to develop the PDF of  $Z_i = Z_{hg,i} e^{j\theta_i}$ , where  $\theta_i \sim U(-q\pi, q\pi)$ . Using the conditional expectation of random variables, we can get

$$f_{Z_i}(x) = \mathbb{E}[f_{Z_i}(x/\theta_i)] = \int_{-q\pi}^{q\pi} f_{Z_i}(x/\theta_i) f_{\theta_i}(\theta) d\theta \quad (49)$$

Using (48), the density function of  $Z_i$  given  $\theta_i$ :

$$f_{Z_i}(x/\theta_i) = e^{-j\theta_i} f_{Z_{hg,i}}(\frac{x}{e^{j\theta_i}}) = \sum_{k_i=0}^{\infty} \sum_{j_i=1}^n \psi_{i,1} x^{-1} H_{1,4}^{3,1} \left[ \zeta_{i,1} \zeta_{i,2} x e^{-j\theta_i} \mid \left( -\beta_{j_i}, \frac{\alpha}{2} \right) \right] \quad (50)$$

We substitute (50) in (49) to get

$$f_{Z_i}(x) = \sum_{k_i=0}^{\infty} \sum_{j_i=1}^n \psi_{i,1} \frac{1}{2\pi j} \int_{\mathcal{L}_i} (\zeta_{i,2} \zeta_{i,1})^{s_i} x^{s_i - 1} \frac{\Gamma(1+\beta_{j_i} + \frac{\alpha}{2} s_i) \Gamma(\beta_{i,1} - \frac{s_i}{\alpha_{i,1}}) \Gamma(\beta_{i,2} - \frac{s_i}{\alpha_{i,2}})}{\Gamma(2+\beta_{j_i} + \frac{\alpha}{2} s_i)} \Gamma(\mu_i + k_i - s_i) (\mathbb{E}[e^{-j\theta_i s_i}]) ds_i \quad (51)$$

Using  $\mathbb{E}[e^{-j\theta_i s_i}] = \frac{\sin q\pi s_i}{q\pi s_i} = \frac{1}{\Gamma(1-qs_i)\Gamma(qs_i)} \frac{\Gamma(qs_i)}{\Gamma(1+qs_i)} = \frac{1}{\Gamma(1-qs_i)\Gamma(1+qs_i)}$  in (51), and applying the definition of Fox's H-function, we get (9), which completes the proof of the theorem.

## APPENDIX B: PDF AND CDF OF $Z_{\text{RIS}}$

The PDF for  $Z_{\text{RIS}} = \sum_{i=1}^N Z_i$  can be computed using the MGF as  $f_{Z_{\text{RIS}}}(z) = \mathcal{L}^{-1} \prod_{i=1}^N M_{Z_i}(s)$ , where

$$\begin{aligned} M_{Z_i}(s) &= \int_0^{\infty} e^{-sx} f_{Z_i}(x) dx \\ &= \sum_{k_i=0}^{\infty} \sum_{j_i=1}^n \psi_{i,1} \int_0^{\infty} x^{-1} e^{-sx} \\ & H_{2,5}^{3,1} \left[ \zeta_{i,1} \zeta_{i,2} x \mid \left( -\beta_{j_i}, \frac{\alpha}{2} \right), (1, q) \right] dx \end{aligned} \quad (52)$$

We expand the Fox's H-function definition and interchange the order of integration (52) to get

$$M_{Z_i}(s) = \sum_{k_i=0}^{\infty} \sum_{j_i=1}^n \psi_{i,1} \frac{1}{2\pi j} \int_{\mathcal{L}_i} (\zeta_{i,2} \zeta_{i,1})^{s_i} \frac{\Gamma(1+\beta_{j_i} + \frac{\alpha}{2} s_i) \Gamma(\beta_{i,1} - \frac{s_i}{\alpha_{i,1}}) \Gamma(\beta_{i,2} - \frac{s_i}{\alpha_{i,2}})}{\Gamma(2+\beta_{j_i} + \frac{\alpha}{2} s_i)} \Gamma(\mu_i + k_i - s_i) \frac{1}{\Gamma(1-qs_i)\Gamma(1+qs_i)} \int_0^{\infty} e^{-sx} x^{s_i-1} dx ds_i \quad (53)$$

The inner integral in (53) can be solved using the identity [42, 3.381.4] as  $\int_0^{\infty} e^{-sx} x^{s_i-1} dx = s^{-s_i} \Gamma(s_i)$ , which can be used to develop MGF in terms of Fox's H-function. Since the MGF of the sum is given as  $M_{Z_{\text{RIS}}}(s) = \prod_{i=1}^N M_{Z_i}(s)$ , the PDF of  $Z_{\text{RIS}}$  can be represented as

$$\begin{aligned} f_{Z_{\text{RIS}}}(x) &= \mathcal{L}^{-1} \prod_{i=1}^N M_{Z_i}(s) \\ &= \sum_{k_1, \dots, k_N=0}^{\infty} \sum_{j_1, \dots, j_N=1}^n \prod_{i=1}^N \psi_{i,1} \frac{1}{2\pi j} \int_{\mathcal{L}_i} (\zeta_{i,2} \zeta_{i,1})^{s_i} \\ & \frac{\Gamma(1+\beta_{j_i} + \frac{\alpha}{2} s_i) \Gamma(\beta_{i,1} - \frac{s_i}{\alpha_{i,1}}) \Gamma(\beta_{i,2} - \frac{s_i}{\alpha_{i,2}}) \Gamma(\mu_i + k_i - s_i)}{\Gamma(2+\beta_{j_i} + \frac{\alpha}{2} s_i) \Gamma(1-qs_i) \Gamma(1+qs_i)} \\ & \left( \frac{1}{2\pi j} \int_{\mathcal{L}} s^{-\sum_i s_i} e^{sx} ds \right) ds_i \end{aligned} \quad (54)$$

Next, we apply the identity [42, 8.315.1] to solve the inner integral as

$$\frac{1}{2\pi j} \int_{\mathcal{L}} s^{-\sum_i s_i} e^{sx} ds = \left( \frac{1}{x} \right)^{-\sum_i s_i + 1} \frac{1}{\Gamma(\sum_i s_i)} \quad (55)$$

Finally, we use (55) in (54) and apply the definition of  $N$ -multivariate Fox's H-function [30, A.1] to get (12). Applying similar steps, the CDF  $Z_{\text{RIS}}$  can be derived using  $F_{Z_{\text{RIS}}}(x) = \mathcal{L}^{-1} \prod_{i=1}^N \frac{M_{Z_i}(s)}{s}$ , as given in (13).

#### APPENDIX C: PDF AND CDF OF UPPER BOUND $Y_{\text{RIS}}$

We use the identity [39, 2.8] to find the  $r$ -th moment of  $Z_i$ :

$$\begin{aligned} \mathbb{E}[(Z_i)^r] &= \int_0^\infty x^r f_{Z_i}(x) dx \\ &= \sum_{k_i=0}^\infty \sum_{j_i=1}^n \psi_i(\zeta_{i,2} \zeta_{i,1})^{-r} \Gamma(\mu_i + k_i + r) \\ &\quad \frac{\Gamma(1 + \beta_{j_i} - \frac{a}{2} r) \Gamma(\beta_{i,1} + \frac{r}{\alpha_{i,1}}) \Gamma(\beta_{i,2} + \frac{r}{\alpha_{i,2}})}{\Gamma(1 + qr) \Gamma(1 - qr) \Gamma(2 + \beta_{j_i} - \frac{a}{2} r)} \end{aligned} \quad (56)$$

Substituting (56) in (20), we get

$$\begin{aligned} f_{Y_{\text{RIS}}}(x) &= \frac{x^{-1}}{2\pi j} \int_{\mathcal{L}} \prod_{i=1}^N \sum_{k_i=0}^\infty \sum_{j_i=1}^n \psi_i(\zeta_{i,2} \zeta_{i,1})^{-r} \\ &\quad \frac{\Gamma(1 + \beta_{j_i} - \frac{a}{2} r) \Gamma(\beta_{i,1} + \frac{r}{\alpha_{i,1}}) \Gamma(\beta_{i,2} + \frac{r}{\alpha_{i,2}})}{\Gamma(2 + \beta_{j_i} - \frac{a}{2} r)} \\ &\quad \Gamma(\mu_i + k_i + r) \frac{1}{\Gamma(1 + qr) \Gamma(1 - qr)} x^{-r} dr \end{aligned} \quad (57)$$

Using (57) in (19) and applying the definition of Fox's H-function, we can get an upper bound on the PDF  $f_{Z_{\text{RIS}}}(x)$  in (21).

Further, using the integral property, the CDF can be computed as  $F_{Y_{\text{RIS}}}(x) = \int_0^x f_{Y_{\text{RIS}}}(u) du$ :

$$\begin{aligned} F_{Y_{\text{RIS}}}(x) &= \frac{1}{2\pi j} \int_{\mathcal{L}} \prod_{i=1}^N \sum_{k_i=0}^\infty \sum_{j_i=1}^n \psi_i(\zeta_{i,2} \zeta_{i,1})^{-r} \\ &\quad \frac{\Gamma(1 + \beta_{j_i} + \frac{a}{2} r) \Gamma(\beta_{i,1} - \frac{r}{\alpha_{i,1}}) \Gamma(\beta_{i,2} - \frac{r}{\alpha_{i,2}})}{\Gamma(2 + \beta_{j_i} + \frac{a}{2} r)} \\ &\quad \Gamma(\mu_i + k_i - r) \frac{1}{\Gamma(1 - qr) \Gamma(1 + qr)} \int_0^x u^{-1} u^r du dr \end{aligned} \quad (58)$$

Thus, using the  $I = \int_0^x u^{-1} u^r du = \frac{\Gamma(r)}{\Gamma(r+1)} x^r$  and substituting (58) in (18), we get (22).

#### APPENDIX D: PDF AND CDF OF SNR WITH DIRECT LINK

Using the PDF of SNR in (27) and expanding the definition of multivariate Fox's H-function, we derive the MGF of  $\gamma_{\text{RIS}}$  as

$$\begin{aligned} M_{\gamma_{\text{RIS}}}(s) &= \sum_{k_1, \dots, k_N=0}^\infty \sum_{j_1, \dots, j_N=1}^n \prod_{i=1}^N \frac{\psi_i}{2} \\ &\quad \frac{1}{2\pi j} \int_{\mathcal{L}_i} (\zeta_{i,2} \zeta_{i,1})^{s_i} \sqrt{\frac{1}{\gamma_{\text{RIS}}}}^{s_i} \\ &\quad \frac{\Gamma(1 + \beta_{j_i} + \frac{a}{2} s_i) \Gamma(\beta_{i,1} - \frac{s_i}{\alpha_{i,1}}) \Gamma(\beta_{i,2} - \frac{s_i}{\alpha_{i,2}}) \Gamma(\mu_i + k_i - s_i) \Gamma(s_i)}{\Gamma(2 + \beta_{j_i} + \frac{a}{2} s_i) \Gamma(1 - q s_i) \Gamma(1 + q s_i)} \\ &\quad \frac{1}{\Gamma(\sum_{i=1}^N s_i)} \left( \int_0^\infty \gamma \sum_{i=1}^N \frac{s_i}{2} - 1 e^{-s\gamma} d\gamma \right) ds_i \end{aligned} \quad (59)$$

where  $\int_0^\infty \gamma \sum_{i=1}^N \frac{s_i}{2} - 1 e^{-s\gamma} d\gamma = (\frac{1}{s})^{\sum_{i=1}^N \frac{s_i}{2}} \Gamma(\sum_{i=1}^N \frac{s_i}{2})$ .

Similarly, to get the MGF for the SNR for direct transmission, we use (30) to get

$$\begin{aligned} M_{\gamma_d}(s) &= \frac{1}{2\sqrt{\gamma_d}} \sum_{j=1}^n B_j \frac{b^{M+m} d^{\frac{a(M+m)}{2}}}{2^{M+m} \Gamma(m) \Gamma(M)} \\ &\quad \left( \sqrt{\frac{1}{\gamma_d}} \right)^{M+m-1} \frac{1}{2\pi j} \int_{L_d} \left( \frac{bd}{2} \sqrt{\frac{1}{\gamma_d}} \right)^{s_d} \\ &\quad \frac{\Gamma(\frac{M-m}{2} - \frac{s_d}{2}) \Gamma(\frac{m-M}{2} - \frac{s_d}{2}) \Gamma(1 - \beta_j - \frac{a(M+m)}{2} + \frac{a}{2} s_d)}{\Gamma(-\beta_j - \frac{a(M+m)}{2} + \frac{a}{2} s_d)} \\ &\quad \left( \int_0^\infty \gamma^{\frac{M+m}{2} + \frac{s_d}{2} - 1} e^{-s\gamma} d\gamma \right) ds_d \end{aligned} \quad (60)$$

where the inner integral is given by  $\int_0^\infty \gamma^{\frac{M+m}{2} + \frac{s_d}{2} - 1} e^{-s\gamma} d\gamma = (\frac{1}{s})^{\frac{M+m}{2} + \frac{s_d}{2}} \Gamma(\frac{M+m}{2} + \frac{s_d}{2})$ . To get the PDF of  $\gamma_{\text{RISD}}$ , we use  $f_{\gamma_{\text{RISD}}}(\gamma) = \mathcal{L}^{-1}(M_{\gamma_{\text{RIS}}}(s) M_{\gamma_d}(s))$  as

$$\begin{aligned} f_{\gamma_{\text{RISD}}}(\gamma) &= \sum_{k_1, \dots, k_N=0}^\infty \sum_{j_1, \dots, j_N=1}^n \sum_{j=1}^n \prod_{i=1}^N B_j \frac{\psi_i}{4\gamma} \\ &\quad \frac{1}{\Gamma(m) \Gamma(M)} \frac{1}{2\pi j} \int_{\mathcal{L}_i} (\zeta_{i,2} \zeta_{i,1}) \sqrt{\frac{\gamma}{\gamma_{\text{RIS}}}}^{s_i} \\ &\quad \frac{\Gamma(1 + \beta_{j_i} + \frac{a}{2} s_i) \Gamma(\beta_{i,1} - \frac{s_i}{\alpha_{i,1}}) \Gamma(\beta_{i,2} - \frac{s_i}{\alpha_{i,2}}) \Gamma(\mu_i + k_i - s_i) \Gamma(s_i)}{\Gamma(2 + \beta_{j_i} + \frac{a}{2} s_i) \Gamma(1 - q s_i) \Gamma(1 + q s_i)} \\ &\quad \frac{\Gamma(\sum_{i=1}^N \frac{s_i}{2})}{\Gamma(\sum_{i=1}^N s_i)} \frac{1}{2\pi j} \int_{L_d} \left( \frac{bd}{2} \sqrt{\frac{\gamma}{\gamma_d}} \right)^{s_d} \\ &\quad \frac{\Gamma(M - \frac{s_d}{2}) \Gamma(m - \frac{s_d}{2}) \Gamma(1 - \beta_j - a(M+m) + \frac{a}{2} s_d)}{\Gamma(-\beta_j - a(M+m) + \frac{a}{2} s_d)} \Gamma(\frac{s_d}{2}) \\ &\quad \left( \frac{1}{\Gamma(\sum_{i=1}^N \frac{s_i}{2} + \frac{s_d}{2})} \right) ds_i ds_d \end{aligned} \quad (61)$$

where we used the following expression:

$$\int_{L} (s)^{-\sum_{i=1}^N \frac{s_i}{2} - \frac{s_d}{2} - \frac{M+m}{2}} e^{s\gamma} ds = \frac{2\pi j \gamma^{\sum_{i=1}^N \frac{s_i}{2} + \frac{s_d}{2} + \frac{M+m}{2} - 1}}{\Gamma(\sum_{i=1}^N \frac{s_i}{2} + \frac{s_d}{2} + \frac{M+m}{2})} \quad (62)$$

Finally, we apply the definition of  $N$ -multivariate Fox's H-function in [30, A.1], to get (31).

To compute the CDF of SNR, we use eq. (31) in  $F_{\gamma_{\text{RISD}}}(\gamma) = \int_0^\gamma f_{\gamma_{\text{RISD}}}(x) dx$  and expand  $N$ -multivariate Fox's H-function in terms of Mellin-Barnes integrals to solve the inner integral as

$$I = \int_0^\gamma x \sum_{i=1}^N \frac{s_i}{2} + \frac{s_d}{2} - 1 dx = \frac{\Gamma(\sum_{i=1}^N \frac{s_i}{2} + \frac{s_d}{2}) \gamma^{\sum_{i=1}^N \frac{s_i}{2} + \frac{s_d}{2}}}{\Gamma(\sum_{i=1}^N \frac{s_i}{2} + \frac{s_d}{2} + 1)} \quad (63)$$

and we apply the definition of  $N$ -multivariate Fox's H-function to get (32).

Similarly, to derive an upper bound for the PDF and CDF of resultant SNR, we use the upper bound for the PDF of  $\gamma_{\text{RIS}}(\gamma)$  in (21) such that

$$\begin{aligned} M_{\gamma_{\text{RIS}}}(s) &\leq \frac{N}{2\gamma} \sum_{k_1, \dots, k_N=0}^\infty \sum_{j_1, \dots, j_N=1}^n \prod_{i=1}^N \psi_i \\ &\quad \frac{\Gamma(1 + \beta_{j_i} - \frac{a}{2} s_i) \Gamma(\beta_{i,1} + \frac{s_i}{\alpha_{i,1}}) \Gamma(\beta_{i,2} + \frac{s_i}{\alpha_{i,2}})}{\Gamma(2 + \beta_{j_i} - \frac{a}{2} s_i)} \frac{\Gamma(\mu_i + k_i + s_i)}{\Gamma(1 + q s_i) \Gamma(1 - q s_i)} \\ &\quad (\zeta_{i,1} \zeta_{i,2}) \left( \frac{1}{N} \sqrt{\frac{1}{\gamma_{\text{RIS}}}} \right)^{s_i} \left( \int_0^\infty \gamma^{N \frac{s_i}{2} - 1} e^{-s\gamma} d\gamma \right) ds_i \end{aligned} \quad (64)$$

with the inner integral as  $\int_0^\infty \gamma^{N \frac{s_i}{2} - 1} e^{-s\gamma} d\gamma = (\frac{1}{s})^{N \frac{s_i}{2}} \Gamma(\frac{N s_i}{2})$ .

Using (64) and (60) in  $f_{\gamma_{\text{RISD}}}(\gamma) \leq \mathcal{L}^{-1}(M_{\gamma_{\text{RIS}}}(s) M_{\gamma_d}(s))$  resulting into an inner integral:

$$\int_{L} (s)^{-N \frac{s_i}{2} - \frac{s_d}{2}} e^{s\gamma} ds = \frac{2\pi j \gamma^{N \frac{s_i}{2} + \frac{s_d}{2} - 1}}{\Gamma(N \frac{s_i}{2} + \frac{s_d}{2})} \quad (65)$$

Using the definition of bivariate Fox's H-function on the resultant expressing comprising (64) and (60) with (65), we can get (31). Similarly, the CDF can be computed as  $F_{\gamma_{\text{RISD}}}(\gamma) \leq \mathcal{L}^{-1}(\frac{1}{s} M_{\gamma_{\text{RIS}}}(s) M_{\gamma_d}(s))$  to get (32), which concludes the proof of the theorem.

#### REFERENCES

- [1] V. K. Chapala, A. Malik, and S. M. Zafaruddin, "RIS-assisted vehicular network with direct transmission over double-generalized gamma fading channels," in *2022 IEEE 95th Veh. Tech. Conf.: (VTC2022-Spring)*, 2022, pp. 1–6.

- [2] Y. Zhu, B. Mao, Y. Kawamoto, and N. Kato, "Intelligent reflecting surface-aided vehicular networks toward 6G: Vision, proposal, and future directions," *IEEE Veh. Technol. Mag.*, vol. 16, no. 4, pp. 2–10, Dec. 2021.
- [3] Q. Wu, S. Zhang, B. Zheng, C. You, and R. Zhang, "Intelligent reflecting surface aided wireless communications: A tutorial," *IEEE Trans. Commun.*, vol. 69, no. 5, pp. 3313–3351, Jan. 2021.
- [4] E. Basar, M. D. Renzo, J. D. Rosny, M. Debbah, M. S. Alouini, and R. Zhang, "Wireless communications through reconfigurable intelligent surfaces," *IEEE Access*, vol. 7, pp. 116753–116773, Aug. 2019.
- [5] D. Kudathanthirige, D. Gunasinghe, and G. Amarasuriya, "Performance analysis of intelligent reflective surfaces for wireless communication," in *ICC 2020-2020 IEEE Int. Conf. Commun. (ICC)*, Dublin, Ireland, July 2020, pp. 1–6.
- [6] Q. Tao, J. Wang, and C. Zhong, "Performance analysis of intelligent reflecting surface aided communication systems," *IEEE Commun. Lett.*, vol. 24, no. 11, pp. 2464–2468, July 2020.
- [7] R. C. Ferreira, M. S. P. Facina, F. A. P. De Figueiredo, G. Fraidenraich, and E. R. De Lima, "Bit error probability for large intelligent surfaces under double-Nakagami fading channels," *IEEE Open J. Commun. Society*, vol. 1, pp. 750–759, May 2020.
- [8] D. Selimis, K. P. Peppas, G. C. Alexandropoulos, and F. I. Lazarakis, "On the performance analysis of RIS-empowered communications over Nakagami-m fading," *IEEE Commun. Lett.*, vol. 25, no. 7, pp. 2191–2195, April 2021.
- [9] M. H. Khoshafa, T. M. N. Ngatched, M. H. Ahmed, and A. R. Ndjiongue, "Active reconfigurable intelligent surfaces-aided wireless communication system," *IEEE Commun. Lett.*, vol. 25, no. 11, pp. 3699–3703, Nov. 2021.
- [10] I. Trigui, W. Ajib, and W.-P. Zhu, "A comprehensive study of reconfigurable intelligent surfaces in generalized fading," [Online], arXiv: 2004.02922, 2020.
- [11] H. Du, J. Zhang, J. Cheng, Z. Lu, and B. Ai, "Millimeter wave communications with reconfigurable intelligent surfaces: Performance analysis and optimization," *IEEE Trans. Commun.*, vol. 69, no. 4, pp. 2752–2768, Jan. 2021.
- [12] V. Jamali, H. Ajam, M. Najafi, B. Schmauss, R. Schober, and H. V. Poor, "Intelligent reflecting surface assisted free-space optical communications," *IEEE Commun. Magazine*, vol. 59, no. 10, pp. 57–63, Nov. 2021.
- [13] V. K. Chapala and S. M. Zafaruddin, "Unified performance analysis of reconfigurable intelligent surface empowered free space optical communications," *IEEE Trans. Commun.*, vol. 70, no. 4, pp. 2575–2592, April 2022.
- [14] H. Du, J. Zhang, K. Guan, B. Ai, and T. Kürner, "Reconfigurable intelligent surface aided TeraHertz communications under misalignment and hardware impairments," [Online] arXiv: 2012.00267, 2020.
- [15] V. K. Chapala and S. M. Zafaruddin, "Exact Analysis of RIS-Aided THz Wireless Systems Over  $\alpha$ - $\mu$  Fading with Pointing Errors," *IEEE Commun. Lett.*, vol. 25, no. 11, pp. 3508–3512, Nov. 2021.
- [16] J. Wang, W. Zhang, X. Bao, T. Song, and C. Pan, "Outage analysis for intelligent reflecting surface assisted vehicular communication networks," [Online], arXiv: 2004.08063, 2020.
- [17] K. Odeyemi, P. A. Owolawi, and O. O. Olakanmi, "Reconfigurable intelligent surface assisted mobile network with randomly moving user over Fisher-Snedecor fading channel," *Physical Communication*, vol. 43, p. 101186, Aug. 2020.
- [18] D. Dampahalage *et al.*, "Intelligent reflecting surface aided vehicular communications," [Online], arXiv: 2011.03071, 2020.
- [19] L. Kong, J. He, Y. Ai, S. Chatzinotas, and B. Ottersten, "Channel modeling and analysis of reconfigurable intelligent surfaces assisted vehicular networks," in *2021 IEEE Int. Conf. Commun. Workshops (ICC Workshops)*, Montreal, QC, Canada, June 2021, pp. 1–6.
- [20] Y. U. Ozcan, O. Ozdemir, and G. K. Kurt, "Reconfigurable intelligent surfaces for the connectivity of autonomous vehicles," *IEEE Trans. Vehi. Technol.*, vol. 70, no. 3, pp. 2508–2513, March 2021.
- [21] A. U. Makarfi, K. M. Rabie, O. Kaiwartya, X. Li, and R. Kharel, "Physical layer security in vehicular networks with reconfigurable intelligent surfaces," in *2020 IEEE 91st Veh. Tech. Conf. (VTC2020-Spring)*, May 2020, pp. 1–6.
- [22] I. Trigui, W. Ajib, W.-P. Zhu, and M. D. Renzo, "Performance evaluation and diversity analysis of ris-assisted communications over generalized fading channels in the presence of phase noise," *IEEE open j. Commun. Soc.*, vol. 3, pp. 593–607, 2022.
- [23] X. Qian, M. Di Renzo, J. Liu, A. Kammoun, and M.-S. Alouini, "Beamforming through reconfigurable intelligent surfaces in single-user mimo systems: Snr distribution and scaling laws in the presence of channel fading and phase noise," *IEEE Wirel. Commun. Lett.*, vol. 10, no. 1, pp. 77–81, 2021.
- [24] D. Li, "Ergodic capacity of intelligent reflecting surface-assisted communication systems with phase errors," *IEEE Commun. Lett.*, vol. 24, no. 8, pp. 1646–1650, 2020.
- [25] T. Wang, G. Chen, J. P. Coon, and M.-A. Badiu, "Study of intelligent reflective surface assisted communications with one-bit phase adjustments," in *GLOBECOM 2020 - 2020 IEEE Glob. Commun. Conf.*, 2020, pp. 1–6.
- [26] P. Xu, G. Chen, Z. Yang, and M. D. Renzo, "Reconfigurable intelligent surfaces-assisted communications with discrete phase shifts: How many quantization levels are required to achieve full diversity?" *IEEE Wirel. Commun. Lett.*, vol. 10, no. 2, pp. 358–362, 2021.
- [27] O. Waqar, "Performance analysis for irs-aided communication systems with composite fading/shadowing direct link and discrete phase shifts," *Trans. Emerg. Telecommun. Technol.*, vol. 32, no. 10, p. 4320, 2021.
- [28] S. A. Tegos, D. Tyrovolas, P. D. Diamantoulakis, C. K. Liaskos, and G. K. Karagiannidis, "On the distribution of the sum of double-nakagami-m random vectors and application in randomly reconfigurable surfaces," *IEEE Trans. Vehi. Technol.*, pp. 1–1, 2022.
- [29] M.-A. Badiu and J. P. Coon, "Communication through a large reflecting surface with phase errors," *IEEE Wirel. Commun. Lett.*, vol. 9, no. 2, pp. 184–188, 2020.
- [30] A. Mathai, R. K. Saxena, and H. J. Haubold, *The H-Function: Theory and Applications*. Springer New York, 2009.
- [31] K. Dovelos, S. D. Assimonis, H. Q. Ngo, B. Bellalta, and M. Matthaiou, "Intelligent reflecting surfaces at terahertz bands: channel modeling and analysis," [Online], arXiv: 2103.15239, 2021.
- [32] M. D. Yacoub, "The  $\kappa$ - $\mu$  distribution and the  $\eta$ - $\mu$  distribution," *IEEE Antennas and Propagation Magazine*, vol. 49, no. 1, pp. 68–81, 2007.
- [33] V. K. Chapala and S. M. Zafaruddin, "Reconfigurable intelligent surface empowered multi-hop transmission over generalized fading," in *2022 IEEE 95th Veh. Tech. Conf.: (VTC2022-Spring)*, 2022, pp. 1–5.
- [34] P. S. Bithas, A. G. Kanatas, D. B. da Costa, P. K. Upadhyay, and U. S. Dias, "On the double-generalized gamma statistics and their application to the performance analysis of V2V communications," *IEEE Trans. Commun.*, vol. 66, no. 1, pp. 448–460, Jan. 2018.
- [35] P. M. Shankar, "Error rates in generalized shadowed fading channels," *Wirel. Pers. Commun.*, vol. 28, pp. 233–238, 02 2004.
- [36] K. Govindan, K. Zeng, and P. Mohapatra, "Probability density of the received power in mobile networks," *IEEE Trans. Wirel. Commun.*, vol. 10, no. 11, pp. 3613–3619, 2011.
- [37] A. Sikri, A. Mathur, and G. Kaddoum, "Joint impact of phase error, transceiver hardware impairments, and mobile interferers on ris-aided wireless system over  $\kappa$ - $\mu$  fading channels," *IEEE Commun. Lett.*, pp. 1–1, 2022.
- [38] H. R. Alhennawi *et al.*, "Closed-form exact and asymptotic expressions for the symbol error rate and capacity of the  $H$ -function fading channel," *IEEE Trans. Veh. Technol.*, vol. 65, no. 4, pp. 1957–1974, 2016.
- [39] A. Kilbas and M. Saigo, *H-Transforms: Theory and Applications*. CRC Press., Mar. 2004.
- [40] Y. Abo Rahama, M. H. Ismail, and M. S. Hassan, "On the sum of independent Fox's  $H$ -function variates with applications," *IEEE Trans. Vehi. Technol.*, vol. 67, no. 8, pp. 6752–6760, 2018.
- [41] I. S. Ansari, S. Al-Ahmadi, F. Yilmaz, M.-S. Alouini, and H. Yanikomeroglu, "A new formula for the BER of binary modulations with dual-branch selection over generalized-K composite fading channels," *IEEE Trans. Commun.*, vol. 59, no. 10, pp. 2654–2658, Oct. 2011.
- [42] I. Gradshteyn and I. M. Ryzhik, *Table of Integrals, Series, And Products*, Jan. 2007.